2-5 Geophysical Interpretation

2-5-1 Method

In the geophysical interpretation it has been on identifying the units based on a combination of their distinctive geophysical characteristics and, where possible, integrating these units within the broad regional stratigraphic framework. Primary subdivision has been largely based on magnetic characteristics apparent in the TMI-RTP and 1VD images, and to a lesser extent the TMI and Analytic Signal images.

2-5-2 Unit Description

The subdivision of units from the geophysical interpretation is listed in Table II-2-1, and illustrated in Fig. II-2-8.

Table II-2-1 Units defined in the geophysical interpretation

Map Unit Code	Description
Undifferentiated Cenozoic Intrusives	
CzIm	Small plugs often with remanent magnetization, intruding Macogon Formation and older sedimentary sequences
CzIr	Composite bodies with reversed remanent magnetization, occasionally positive outer margins or high potassic zones (CzIr-k)
CzIp	Small magnetic plugs and domes. Possibly some associated with former volcanic centers; some with high K suggests felsic character. Intruding Susungdalaga Volcanics
CzIg	Early Cenozoic granodiorite/diorite with moderate K response and non-magnetic character
Pleistocene Labo Volcanics	
QLpf1 and Qlpf2	Andesitic to dacitic pyoclastic flows, non-magnetic, includes most recent units around summit and north side of Mount Labo, and a tongue of older high Th flow unit to southwest. Shown as overlay unit to geomagnetic units described below.
QLcc	Moderately to highly magnetic lava flows, probably andesite
QLbum	Moderately magnetic volcanic unit including lava, older than QLcc
QLbun	Weakly to non-magnetic volcanic unit, including altered and weathered lava and/or pyroclastic, with minor magnetic highs due to small domes, plugs and magnetic lava flows
QLdd	Magnetic (high) andesite lava domes and/or high level intrusives, some with K-alteration haloes or associated zones
Pliocene Susungdalaga Volcanics	
PSvc	Area of radiating magnetic (high) flows, ? around older volcanic center
PSvm	Magnetic (high) volcanic, composite unit with dipping sheets, probably andesite
PSvn	Weakly to non-magnetic weathered and/or altered volcanic including

Map Unit Code	Description
	pyroclastic, relatively homogeneous magnetic character
PSvr	Similar to PSvn but remanently magnetized, i.e. weakly to non-magnetic weathered and/or altered volcanic including pyroclastic, relatively homogeneous magnetic character
PSvh	Heterogenous volcanic unit, including horizons with remanent magnetization
PSva	Pervasively altered volcanic, expressed as subdued magnetic response and associated high K signature
Pliocene Macogon Formation	
PMm	Volcanic-dominated unit with moderate to high degrees of magnetization, high-frequency anomalies due largely to normally magnetized bodies, NW trends with cross cutting NE-trending dykes, moderate to high Th response
PMmm	Volcanic unit with moderate magnetic response, NW trends, moderate to high Th response
PMa	Magnetite-depleted corridors associated with NW faults
Miocene Bosigon Formation	
MBm	Moderate to high magnetic response due to basaltic units, high K due to sedimentary component?, NW trends, cut by NE-trending dykes
MBn	Altered magnetite-depleted zones
Cretaceous Tigbinan Formation	
KTm	Volcanic (basaltic) bearing unit with linear magnetic anomalies (moderate) and low potassium
KTmk	Mixed volcanic-sedimentary unit with linear magnetic anomalies (moderate) and variable to high potassic response, alteration produces variable response
KTn	Subdued magnetic response associated with sedimentary dominated sequence
KTnk	Subdued magnetic response associated with sedimentary dominated sequence similar to KTn, but with higher K response

(1) Labo Volcanics

The youngest geophysical unit is the Labo Volcanics, which has been subdivided into units with geophysical characteristics broadly consistent with the geological members (Table II-2-1). The Labo Volcanics are confined to the east of the study area. Their western boundary approximates to the course of the Labo River, whereas to the south the boundary with the older Susungdalaga Volcanics is more uncertain, and is based largely on the gamma-ray spectral signature.

The four units defined on geophysical characteristics are in part overlain by pyroclastic flows (QLpf) which lack a magnetic expression. To the north of Mount Labo and around the summit, these form a blanket distinguishable on the Landsat image and forming a broad tongue extending to the north beyond the study area (Fig. II-2-8). Approximately 9 km SW of Mount Labo, the toe of an older more felsic flow is suggested in the Landsat and Thorium/Uranium data, again this unit is transgressive to the underlying geomagnetic units.

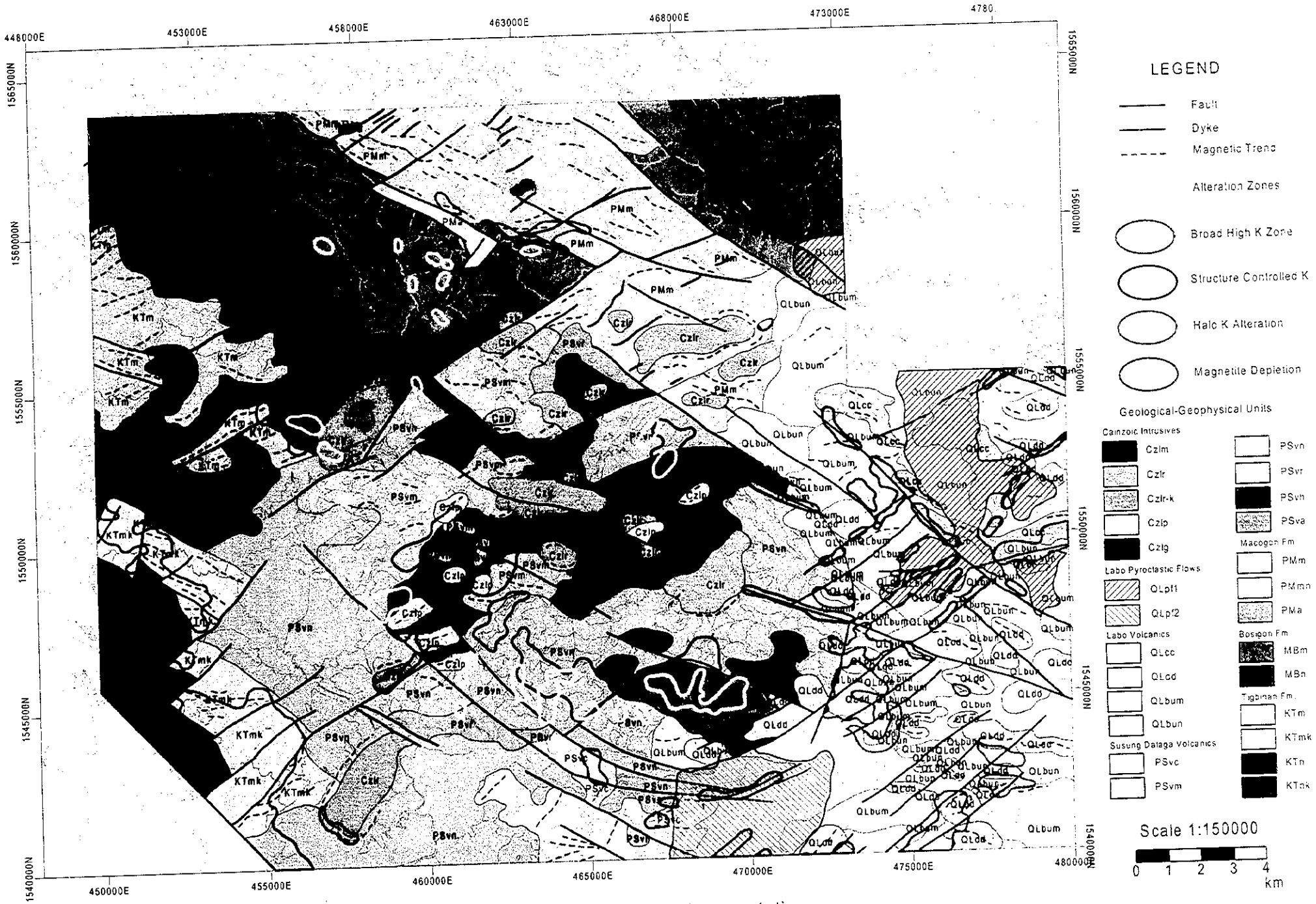

Fig. II-2-8 Geophysical Interpretation

The geophysical units delineated in the Labo Volcanics, excluding QLpf (Table II-1-1) are based largely on magnetic properties (Fig.II-2-8). The youngest units represent magnetic lava, probably andesite, and possible associated feeder zones on the crest and northern flanks of Mount Labo (QLcc). Occurrences of the less coherent magnetic unit Qlbum are composite, probably comprising a series of inter-layered lavas and units of moderate to high degrees of magnetisation. Lava dome units (QLdd) on the south flank of Mount Labo and also to the northeast, form discrete magnetic highs and recognisable topographic highs in the Landsat image (Fig.II-1-1). The domes generally have a low radiometric signature, but some have haloes of potassic alteration (Fig. II-2-4) indicative of probably now extinct marginal geothermal systems generated by the heat associated with their intrusion. Magnetic modelling (Appendix 11) suggests that some of these so-called lava domes are quite thin and may represent dissected remnants of lava flows rather than isolated domes. Unit Qlbun probably comprises weathered and/or altered volcanics including pyroclastic horizons, and is either non-magnetic or weakly magnetic, though dispersed anomalies of high amplitude are due to small domes or andesitic lavas which have not been mapped individually.

The Labo Volcanics have a low background thorium and uranium signature in contrast to the older Pliocene volcanics (Figs. II-2-5, II-2-6). However the potassic response over Mount Labo is more variable due to a combination of alteration, and detrital material eroded from areas of alteration and now concentrated along stream and river courses. Alteration zones include those described by Zaide-Delfin et al (1995) associated with hot springs along fault zones. Recent drainages incising through the blanket of most recent pyroclastic flows on the northern flank of Mount Labo, are also characterised by a high potassic signature. Uranium displays a weak positive correlation with potassium, with alteration zones having a weakly elevated response.

(2) Susungdalaga Volcanics

This volcanic unit not only forms a broad plateau in the centre of the area, but also a lower topographic area in the south presumably due to the dominance of softer more easily weathered pyroclastic dominated units (Figs.II-1-1, Fig.II-2-8). Subdivision of the Susungdalaga Volcanics is largely on its magnetic character, which is similar to parts of the Labo Volcanics. Numerous short strike-length magnetic linears of high magnetic amplitude, and linears of variable orientation reflect a heterogenous combination of lava flows, lava domes and dykes in less magnetic host lithologies. Significant areas of subdued magnetic character are also present, both on the plateau area and to the south.

The area dominated by the more magnetic units, and having a similar magnetic expression as the Pleistocene Labo Volcanics, is associated with the plateau in the centre of the study area. Hence this area may represent the eroded roots of an older volcano. A ring of magnetic highs, associated discrete magnetic anomalies and K-alteration near Susungdalaga Mountain (Fig. II-2-2, II-2-8) may represent a former eruptive centre. To the east a prominent circular feature outlined by a combination of magnetic data and topographic features may indicate a second centre approximately midway between Susungdalaga Mountain and Mount Labo (centred on approximately 468500 mE, 1550000 mN). In the south, a set of radiating magnetic anomalies is indicative of a possible small centre (located at approximately 465000 mE, 1540000 mN) expressed largely as a series of radiating magnetic lavas, this would have been subsidiary to the main volcanic complex to the north.

Thus the Susungdalaga Volcanics comprises a heterogeneous sequence of magnetic volcanics, lava domes, dykes and other intrusives centred around two main eruptive centres, passing outward into pyroclastic-dominated sequences which have a more subdued magnetic expression and also form the topographically lower areas.

The gamma-ray spectral signature of the Susungdalaga Volcanics is characterised by highly variable potassium gamma-ray spectral values and relatively uniform elevated thorium and uranium, especially in the more lowland areas in the south. The variability potassium is due in part to the distribution of alteration. Both the Labo and Susungdalaga Volcanics contain largely intermediate volcanics, hence an increased felsic character is unlikely to account for the higher uranium and thorium gamma-ray spectral values in the latter. However, weathering of intermediate volcanics can increase their thorium and uranium contents (Dickson and Scott, 1997) and this may account for the higher spectral response for uranium and thorium.

Prominent alteration within this unit is present along the southern margin of the central plateau where it has been mapped along stream courses from the Alawihaw alteration zone to the Baliwag alteration zone. It is also expressed as highs in the potassium gamma-ray spectral data, however, at its eastern end it may in part relate to the present geothermal system on the southwestern flank of Mount Labo. Elsewhere it is interpreted to be related to older systems associated with eruptive centres of the Susungdalaga sequence.

(3) Macogon Formation

This dominantly volcanic unit is present in the north of the study area where it has been subdivided into two broad groupings. PMmm has a uniformly high magnetic signature presumably due to the dominance of andesitic lavas, whereas PMm which has more discrete magnetic units, possibly due to dispersed magnetic lava flows within a sequence with dominated by non-magnetic pyroclastic and/or sedimentary units. Both units are characterised by northwest trends (Figs.II-2-2, Fig.II-2-8) associated with the individual magnetic volcanic units, whereas cross-cutting northeast trends are interpreted to represent mafic dykes. The moderate to high thorium and uranium signature may be the result of a greater degree of weathering of this unit as compared with the younger Labo Volcanics.

High potassic zones within the Macogon Formation are considered to reflect potassic rich alteration. For example, around the Nalesbitan prospect the argillic alteration forming the halo to the mineralisation is outlined by a discrete potassium high. Uranium may also be weakly elevated in these zones. An irregular high potassic zone to the east of Nalesbitan is also considered to be alteration.

A broad corridor of low magnetisation east of Nalesbitan and bounded by northwest trending faults is interpreted as a broad zone of demagnetisation. However, only limited potassic alteration is associated with one of the bounding faults.

Definition of the contact with the Susungdalaga Volcanics to the south is difficult, however, the latter is characterised by a more heterogeneous magnetic character, and lacks the more linear generally NW-trending magnetic features which are present in the Macogon Formation. Neither the radiometric nor Landsat data assist in defining the boundary.

The dominant northwest trends within the Macogon Formation and suggestions of a broad open synform (Sillitoe et al, 1990) may indicate that the Macogon Formation has experienced weak

deformation and is thus older than the undeformed Susungdalaga Volcanics to the south. The greater continuity and regularity of units in the Macogon Formation may also be due to deposition, at least in part, in a subaqueous environment by contrast to the subaerial setting of the Susungdalaga and Labo Volcanics.

(4) Bosigon Formation

This unit has been interpreted in the northeast and northwest of the study area based on a combination of moderate magnetic response, low thorium and uranium, and moderate to high potassium signatures. The low thorium and uranium values distinguish the Bosigon Formation from the overlying Macogon Formation, the contacts with which are both unconformable and structural. The linear magnetic trends within the Bosigon Formation are presumed to relate to interlayered basalt units within the sedimentary sequence, with the sediments contributing to the higher potassic values.

(5) Tigbinan Formation

The western portion of the survey area is interpreted to comprise sedimentary dominated sequences of the Cretaceous Tigbinan Formation and also possibly the Miocene Santa Elena Formation. For convenience, the geomagnetic units present have collectively been assigned to the Tigbinan Formation.

Intercalated andesite, spilite, and sediments (units KTmk and KTm) with linear magnetic trends (moderate intensity) can more confidently be assigned to the Tigbinan Formation. These two units, KTmk and KTm, are distinguished on their potassium signature with KTmk having a variable and often high potassium response, whilst KTm is lower in potassium, uranium and thorium. The variability of the response in both magnetic and gamma-ray spectral data for KTmk, even for a single geomagnetic unit, may be due to both weathering and irregular cover of younger sediments/units. This is supported by the Landsat data.

The remaining units (KTn and KTnk) represent sedimentary rocks dominated units with a low magnetic response, and they are distinguished on the basis of a higher potassic signature for KTnk. Both units have low uranium and thorium gamma-ray spectral values. The presence of more finer grained clay rich clastic material present in KTnk may account for the higher potassic character in comparison with more mafic volcaniclastic debris and/or coarser sediments in KTn.

(6) Cenozoic Intrusives

Several distinct geophysical phases have been identified (Table II-1-1, Fig. II-2-8).

- Small circular, plug-like bodies (CzIm) with both highs and lows in TMI data indicating both remanent and normal magnetization, and intruding the Macogon Formation. One of the most prominent bodies is centered near 456 100 E and 1 557 000 N and is characterized by a very discrete thorium-uranium anomalies, a magnetic high in TMI-RTP data, but no distinctive potassium signature indicating an intermediate body possibly alkaline (sodic) in character. A second anomaly at 451100 E and 1561700 N has a more subdued and composite thorium and uranium anomaly.
- Larger, often elongate bodies (CzIr) up to 3.8 km in length are defined by magnetic highs in TMI and lows in TMI-RTP, indicating reverse polarization due to remanent magnetization.

Modelling suggests they are composite in character. They are distributed through the center of the area intruding the Macogon Formation and Susungdalaga Volcanics. These bodies have no distinctive response in the gamma-ray spectral data, apart from a high potassic core in a body approximately 6 km northwest of Susungdalaga Mountain. This body also has a normally magnetized rim indicating a zoned body and cooling through a magnetic polar reversal. The age of these intrusives is unknown, other than a lower limit for the emplacement age which is controlled by geochronology for the host Susungdalaga Volcanics (3.45 – 4.32 Ma).

- Smaller discrete positive magnetic highs within the Susungdalaga Volcanics may be small plugs and lava domes (CzIp) similar to those within the Labo Volcanics. Some have high potassium gamma-ray spectral response, especially two of three bodies southeast of Menato Susungdalaga.
- East of Mapalot, a larger, older intrusive with low magnetic response (CzIg) may correspond to a granodiorite referred to by Mitchell and Leach (1991) and Sillitoe et al (1990). A moderate potassic response supports the felsic character.

In addition, magnetic dykes of relatively short strike length are shown on Fig.II-2-8, but are not mapped as discrete bodies. These largely intrude the Macogon Formation and northern areas of the Susungdalaga Volcanics and may equate to the andesite porphyry dykes described by Sillitoe et al (1990).

2-5-3 Alteration zones

Possible alteration zones as illustrated in Fig.II-2-4, largely comprise areas of potassic alteration identified from the gamma-ray spectral data, as well as areas of alteration mapped by this field.

The alteration zones mapped by this field survey are associated with broad highs in the potassium gamma-ray spectral data, these are more extensive than the zones mapped along streams (Fig.II-2-4). Uranium may also be weakly elevated hence the pink rather than red hues of these zones in Fig.II-2-7. In the Alawihaw – Kilbay Creek area, a broad diffuse potassic high (about 3 km in extent) extends outside of the creek system and generally upstream of the major creek junction. Some potassium anomalism following the creek downstream is probably largely due to alluvial detritus along the creek bed. An associated broad magnetic low suggests significant demagnetization associated with the potassic alteration.

To the west alteration in the Layaton Malaki Creek area (4.5 km west of the Alawihaw – Kilbay Creek area) is expressed as a broad 3km wide zone high potassium gamma-ray spectral values extending east and northwest of the creek system. This area occurs within a more extensive area of homogeneous but moderate magnetic response that does not appear the relation to the alteration system. To the west again the more linear zone defined as the Susungdalaga Mountain south area (2 km south of Susungdalaga Mountain itself), contains a corridor of alteration extending upstream of and peripheral to the mapped area. The WNW-trending fault systems referred by JICA and MMAJ (1999) may relate to the major NW-trending fault interpreted in this area in the magnetic data that do not however otherwise reveal the alteration.

To the northwest, broad zones of potassic alteration define a 3-3.5 km halo around Susungdalaga Mountain coincident with an inferred older eruptive center. The elevated potassium response suggests more extensive alteration than that indicated by the limited creek-bed mapping. The lack

of expression of this alteration in the underlying magnetic data suggests however that this alteration may define only limited hydrothermal systems. Two kilometers to the southwest, two highs in potassium data are related to two inferred high-level intrusives (Czlp) rather than alteration.

None of the above areas have any particular expression in the available Landsat data images. They do, however, form a broad NW-trending corridor of alteration, 3-4 km wide and 12 km in length, bracketed between major west-northwest to northwest trending fault sets, the southern or southwestern set passes through Menato and the northern or northeastern set passes north of Susungdalaga Mountain.

On the flanks of Mount Labo a number of linear highs in the potassium data are associated with geologically mapped structures Zaide-Delfin (1995), at least some of which have active geothermal springs with known alteration zones. Some of these linear features also follow deeply dissecting drainages on Mount Labo (compare Figs 18 and 20), reflecting a combination of fault control on drainage, concentration of eroded altered material along the drainage, and exposure of altered material within drainages. These zones of alteration are more localized than those in the Alawihaw – Kilbay to Susungdalaga Mountain area, and are probably directly related to hydrothermal activity being generated by magma sources still present below or formerly present below Mount Labo. They relatively focused within active or recently active fault systems.

On a local scale, potassium-rich alteration is also associated with some of the lava domes on the south side of Mount Labo, presumably resulting from contemporaneous hot fluid circulation generated in association with their formation (e.g. 474000 mE, 1544000mN).

A broad, high potassium (weak uranium) anomaly at Nalesbitan is associated with the halo of argillic alteration around the orebody. It is broadly elongate extending for about 2.5 km parallel to the dominant structural trends, supporting structural control on mineralization and alteration. Similar elongate zones are present on the northern margin of the study area. The signature of Nalesbitan Prospect in the Landsat 543 band combination image (Fig. II-1-1) is due to vegetation clearing around the prospect rather than the primary alteration system. At the scale of the data, the area of alteration indicated by the potassium gamma-ray spectral data, does not equate to a distinctive magnetic response. However interpreted fault associated magnetite depleted corridors occurs to the northeast and possibly southwest. East of Nalesbitan Prospect, an irregular area of high potassium values is closely associated with intersecting northwest and northeast faults suggesting a strong structural control, but alteration appears less pervasive than that at Nalesbitan.

The origin of a broad potassium high southwest of Nalesbitan Prospect (centered near 456500 mE and 1554800 mN) is associated with the argillic zone of the Katakian alteration zone. It is situated adjacent to a major NE-trending fault with intrusives to the east and north.

Southwest of Mount Labo on the southern edge of the study area (eastings of 469000 mE and 472000 mE), are two broad regions of high potassium gamma-ray spectral values. Their forms however suggest a close relationship to NE-trending faults and topographic lineaments. The western region occurs in the toe of an inferred relic pyroclastic flow unit, and may represent alteration associated with "degassing" from this unit. The eastern region is associated with faults cutting an inferred high-level intrusive or lava dome, and alteration may be related to fluids sourced from the body and focused into the NE-trending faults.

In the southwest of the survey area, a zone of higher potassium gamma-ray spectral response extending from Mapulot to Del Gallego, broadly correlates with higher uranium and thorium values in the gamma-ray spectral data, and a unit with linear magnetic anomalies in the Tigbinan Formation. The elevated gamma-ray spectral response of this unit may be due to a combination of alteration, weathering and lithological control.

2-5-4 Structure

The magnetic interpretation (Fig. II-2-2) and the DTM data (Fig. II-2-1) both highlight the dominant NW and NE-trending structural fabric of the area. These fault sets are interpreted to relate to the larger-scale tectonic setting of oblique convergence and associated sinistral movement on the NW-trending trending Philippines Fault to the west of the survey area. The WNW-ESE trending Legazpi Lineament further to the south on Bicol Peninsula has in part controlled activity of the active Mayon Volcano. Parallel structures are present on Mount Labo, and this regime may have also produced the broad WNW elongation of lava domes within the Labo Volcanics. The NE-trending faults indicate largely dextral movement with vertical normal faulting being characteristic of the WNW-trending structures.

Older dyke swarms with dominant NE trends largely intruding the Macogon Formation are orthogonal to the current extensional direction, suggesting a different tectonic regime late in the magmatic event associated with these Macogon volcanisms. The broadly synformal character and dominant NW-trending volcanic units in the Macogon Formation are compatible with this setting.

2-6 Discussion

The level of exposure of the volcanic sequence is largely at e.g. on Mount Labo, or within a few hundreds of metres of the current or palaeo-landsurface. Although deeper erosional levels occur over the Bosigon Formation in the northeast and older Cretaceous sediments in the west, their current level is also probably close to the palaeosurface during the periods of active volcanism in the area. Hence, the primary target is likely epithermal precious metal mineralisation with the level of exposure generally too high for porphyry-style mineralisation. This does not preclude the possible existence of porphyry Cu/Au systems at depth (2-3km) beneath the epithermal, high-sulfidation Au mineralisation which represents the upper levels of a high-sulfidation hydrothermal system according to the model of Corbett and Leach (1994). In this model porphyry-style mineralisation forms proximal to the intrusive driving the system, whilst epithermal style mineralisation forms at higher levels with a strong structural control.

Although examples of proximal gold deposits and porphyry copper deposits occur in the Philippines, most of those are not considered to be genetically related. The gold deposits are typically Pliocene or younger (e.g. Nalesbitan) and exhibit a close spatial relationship with recent arcs. Porphyry copper deposits are typically at least Miocene in age, and are associated with either older equivalents of these arcs or now extinct arcs (Mitchell and Leach, 1991). The absence of significant pre-Pliocene magmatic activity in the survey area thus also reduces the potential for porphyry style mineralization.

Nalesbitan Prospect, a high sulfidation epithermal gold deposit, represents the only significant known mineralization in the area. It is characterized by an association with NW-trending faults, with mineralization possibly being focused in dilational zones within these faults, and a halo of

argillic alteration expressed as high potassium in the gamma-ray spectral data.

Important factors in the exploration for epithermal mineralization (White and Hendenquist, 1990) are as follows:

- distribution of intrusives deep below the surface to provide heat for meteoric water circulation and to contribute magmatic components to the system
- presence of favorable structural settings –mineralization is commonly on subsidiary structures rather than the prominent regional features
- presence of extensive areas of alteration as these are commonly associated with the upper levels of geothermal systems, and, in particular, which associated with structures considered favorable
- geochemical anomalism

Geophysical data can be used to identify several of these parameters especially at a regional scale, however detailed prospect evaluation e.g. outlining specific ore hosting alteration and structures, may not be possible as these represent only a small part of the alteration system.

By using Nalesbitan Prospect as a case study, the interested areas are considered to be those showing a combination of NW-trending structures and alteration expressed as high potassium in the gamma-ray spectral data. In addition, Sillitoe et al (1990) describe a pyroxene andesite plug or dome southeast of the mineralization. This body appears to be too small to identify with certainty in the magnetic data, however, potentially larger plug type intrusives are present northeast of the mineralization.

To the east of Nalesbitan, potassic alteration centered on the Salobosogin-Yakalan alteration, has a strong structural control, with both NW- and NE trending faults. The NW control, at the proximity to Nalesbitan, and the presence of an interpreted intrusive approximately 1 km to the north (indicative of intrusive activity in the area rather a specific mineralizing body) suggest that this zone has some potential.

A broad potassic high southwest of Nalesbitan at the Katakian alteration zone 456000 mE and 1554800 mN is associated with NE-trending faults rather than NW-trending, but is proximal to major intrusive bodies.

The another main interested area is the NW-trending regional corridor of zones of alteration zones extending from the Alawihaw – Kilbay Creek area to the Tonton River area. The northwestern end of this corridor is potentially of the most interest due to the presence of a number of interpreted intrusives. This study supports the interest in the area which mapped alteration along the drainages and outlined anomalous gold and minor copper, and also indicates the alteration is much more extensive than indicated by the previous mapping, thus increasing the potential of the area.

Alteration systems on Mount Labo are part of currently and recently active geothermal systems. The alteration is currently focused along fault systems along which the geothermal systems are upwelling. Minor base metal anomalism is present at depth. The current level of exposure is high in the geothermal system. The dominance of the expression of shallow sourced high frequency anomalies in the magnetic data means that any deeper intrusives (>300-400 m) that may be driving the current geothermal systems on Mount Labo cannot be readily delineated.

The nature of high potassic zones in older sediments in the west of the area is uncertain. These may have a greater lithological control, but no geochemical data or field observations of lithologies

present are available to support either a lithological or alteration control. Potentially this high-K signature may represent alteration systems distal to former eruptive centers in the Susungdalaga Volcanics, although there are no indications in the magnetic data of coeval intrusives which may have driven the hydrothermal system.

2-7 Summary

The magnetic data as TMI-RTP are characterized by high frequency responses due to shallow magnetic volcanic units. The majority of these are due to induced or normally magnetized bodies producing highs in the TMI-RTP, and dipolar anomalies with a dominant low in the TMI data. However, several negative anomalies in TMI-RTP indicate remanent, reversely magnetized bodies (Fig.II-2-2). The geomagnetic units are often composite, however, data are not sufficiently detailed to map out the thin individual volcanic units. Many are portrayed as trend lines, these are shown where the trends are continuous for more than 600-700 m, i.e. across several flight lines.

The Landsat and DTM data clearly outline the dissected form of the now extinct strato-volcano of Mount Labo. No other obvious volcanic centers are apparent in this topographic data, although the broad plateau west of Mount Labo may represent the eroded roots of an older system. Magnetic modelling suggests former centers within the Susungdalaga Volcanics including one just north of Susungdalaga Mountain.

The dominant contribution of surface or near-surface magnetic sources is supported by the magnetic modelling. However over Mount Labo, the Landsat data outline the presence of a surface blanket of dissected pyroclastic flows (Fig.II-1-1) which are non-magnetic and form a thin cover over the underlying magnetic units that include andesitic lava.

The radiometric data, especially potassium, has been used where appropriates to further discriminate the geomagnetic units as well as to outline zones of alteration. The potassium gamma-ray spectral response is due to a number of factors, including lithology, potassic alteration and the degree of exposure. Alluvial material can produce a high response due to a combination of the response of source material and high exposure. For example, the Labo River has a characteristic high K signature due to these factors (Fig.II-2-4).

The magnetic data may also outline areas of alteration. These may be zones of low magnetic response due to magnetite destruction during hydrothermal alteration, as distinct from lows due to reversely polarized bodies referred to above. A map showing the distribution of alteration has been produced separately from the representation of geomagnetic units (Fig.II-2-2, Fig.II-2-7).

The thorium and uranium gamma-ray spectral data show similar patterns and reflect a broad lithological control. Pleistocene volcanics of Mount Labo have a low uranium –thorium response along with sediment-dominated sequences of the Bosigon Formation in the northeast, and the Tigbinan and Santa Elena Formations in the west. In contrast, the Miocene Macogon and Susungdalaga Volcanics through the center of the area have a higher response (Figs.II-2-5, II-2-6).

The ternary radiometric image (Fig.II-2-7) is broadly divisible into areas with lower uranium and thorium, and higher potassium with pink hues in the east and west, and a broad zone with higher uranium and thorium with cyan hues in the center. This central area is associated with Pliocene volcanics, local white to pink hues within it represent areas of alteration and/or high potassic lithologies.

Chapter 3 Geochemical Survey of the Stream Sediments Samples

3-1 Sampling

The stream sediments samples were collected at the junction of main river and tributary. Samples were taken by 30 mesh sieves in the field and stored into craft bags. At the base-camp after drying, the samples for the ordinary geochemical analysis were sieved by 80 mesh sieve, and shipped to the laboratory. The samples for the BLEG analysis were shipped without sieving after drying. The amount of each BLEG sample was more than 2 kg.

The number of the ordinary geochemical samples is 289, including 18 duplicated samples. The number of the BLEG geochemical samples is 35.

The locations of the stream sediments samples are shown in Appendix 2. The results of chemical analysis are shown in Appendix 6 and Appendix 7.

3-2 Geochemical Interpretation

3-2-1 BLEG analysis

The histograms and probability plots of Au and Cu values are shown in Fig.II-3-1. It is clear that the distributions of both Au and Cu data are bi-modal. These two populations can be interpreted as "background" population and "anomaly" population. Threshold values of Au and Cu are 10 ppb and 0.5 ppm respectively. The anomaly distribution charts with raw values are shown in Fig.II-3-2.

[Au] The high Au values are concentrated at the drainage areas of Nalesbitan and Tuba gold deposits. It might reflect the contamination of present small-scale mining activity. Other anomaly values are associated with the Alawihaw-Bacoco alteration zones in the eastern part of Kilbay River and the drainage of the Katakian alteration zone. In the Layaton Creek – Kampusta alteration zones, Au values are ranging from 2 to 4 ppb, which are slightly high but not anomalous values.

[Cu] The high Cu values are concentrated at the drainage area of Nalesbitan and Tuba gold deposits, and the broad area in Kilbay valley. The later is associated with the alteration zones on the south of Susungdalaga Mountains.

3-2-2 Ordinary geochemical analysis

(1) Statistical processing

A common logarithm value of each analysis value is used for data processing. As for an analysis value lower than detection limit value, a half of that value is adopted in the statistical processing. Also as for an analysis value higher than a maximum detection limit value, the limit value is adopted.

Table II-3-1 shows statistical values of each element. The histograms and probability plots of each element are shown in Fig.II-3-3. The class interval of histogram is 1/2 of a standard deviation (σ). The values of Bi, Ti, U and W show only the values below the detection limit value.

The covariance and correlation coefficient matrix of each element are shown in Table II-3-1. The calculation of correlation was done for 27 elements. The elements that have more than 95% values of the below detection limit are excluded.

The elements associated with Au and Cu mineralization are expected high positive correlation with Au and Cu. These elements are Au, Ag, As, Cu, Hg, Mo, Pb, S and Sb. Therefore the distributions of these elements are shown in Fig.II-3-4~II-3-8.

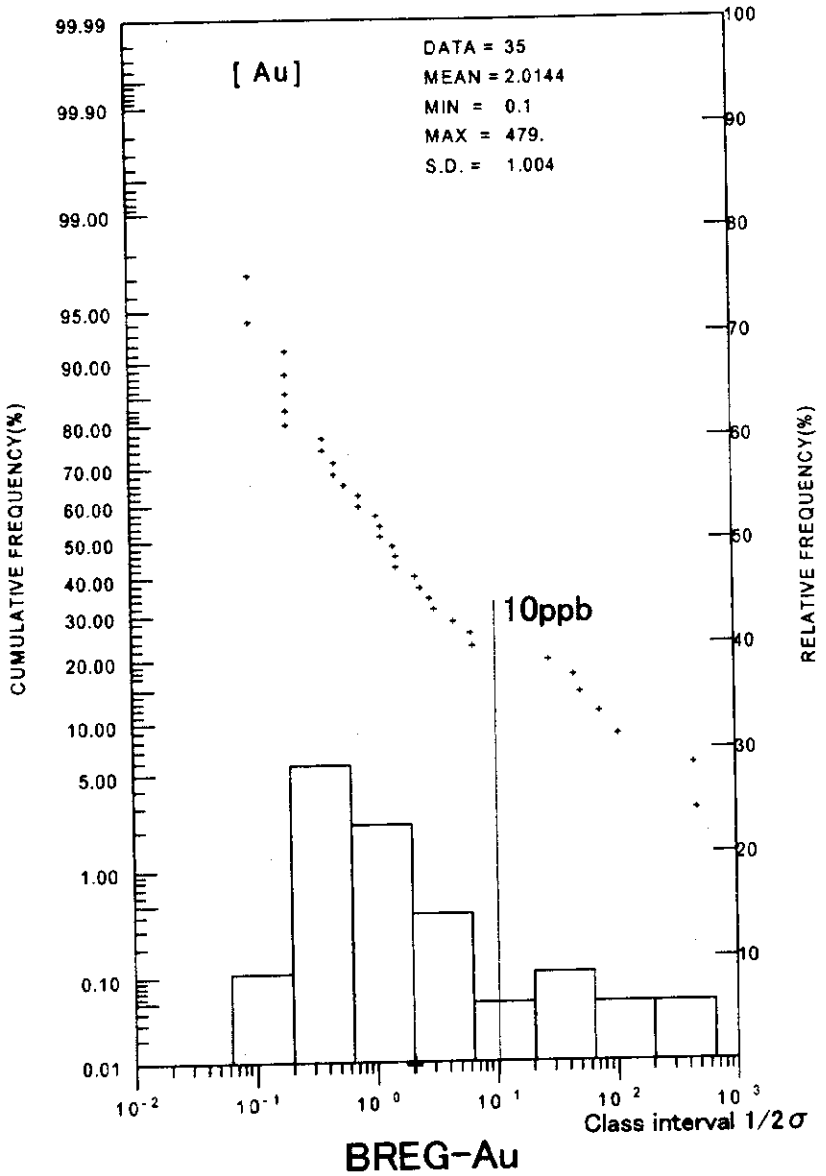

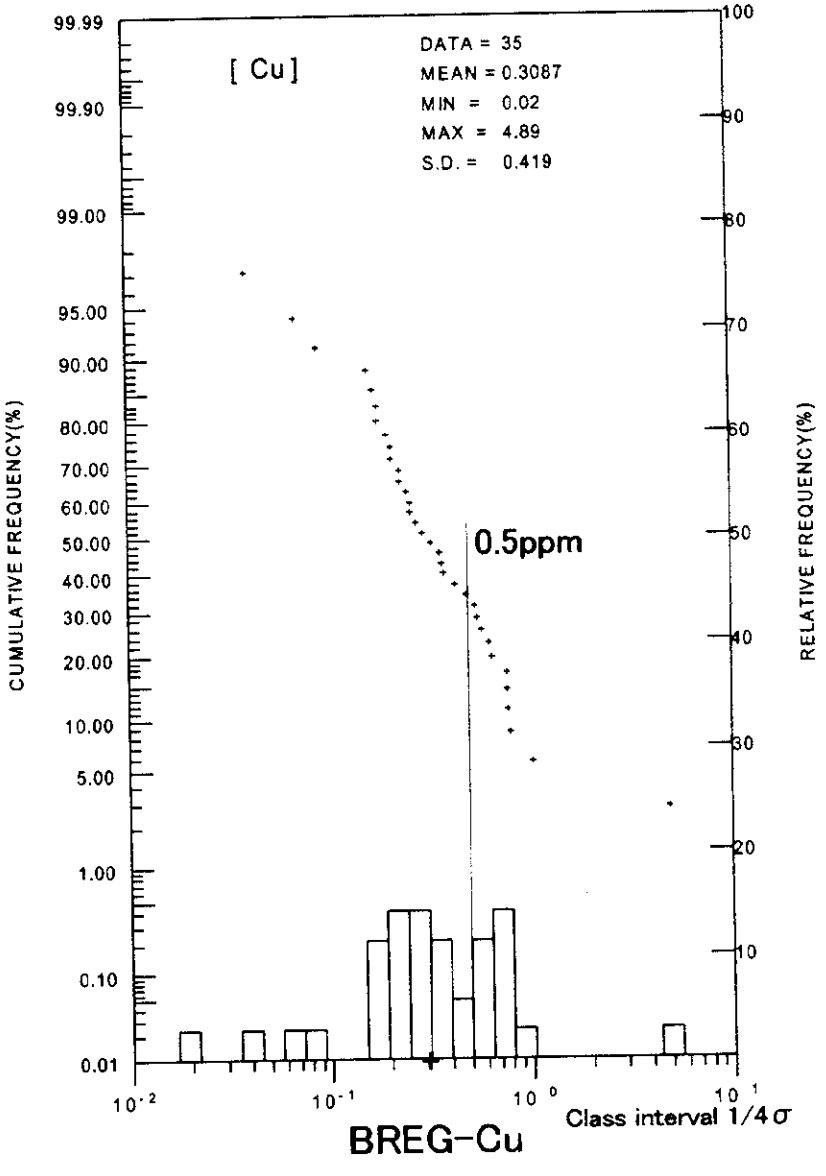

Fig. II-3-1 Probability Plot of the BLEG Samples

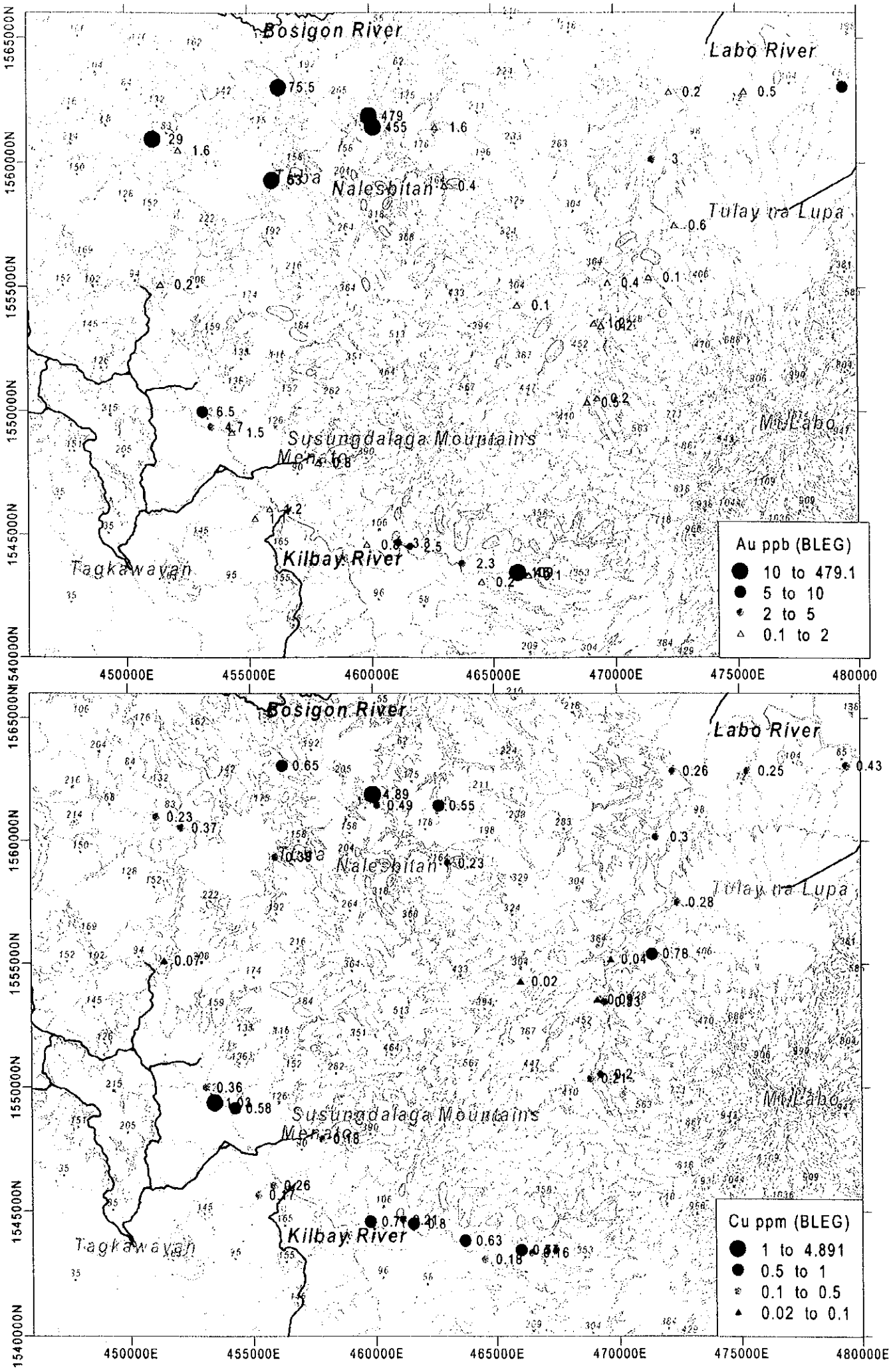

Fig. II-3-2 Au and Cu Content of the BLEG Samples

Table II-3-1 Basic Statistics and Correlation Coefficient of the Stream Sediments Samples

Original Data Infomation　　Number of Component : 27
Number of Sample : 289

Result of Statistics (Logarithmic)

Elements	Au	Ag	Al	As	Ba	Bi	Ca	Co	Cr	Cu	Fe	Hg	K	Mg	Mn	Mo	Na	Ni	P	Pb	S	Sb	Sc	Sr	Ti	V	Zn
Max_val	4.286	1.593	0.709	3.260	2.672	2.072	0.155	1.771	2.605	3.675	1.176	4.324	-0.921	0.450	3.362	1.580	-1.301	2.728	3.155	2.547	0.549	2.723	1.415	2.354	-0.201	2.863	2.398
Min_val	-0.301	-1.000	-0.523	0.000	-0.301	0.000	-2.000	-0.301	0.477	0.477	0.065	0.699	-2.000	-2.000	1.398	-0.301	-2.000	0.000	1.778	0.000	-2.301	0.000	0.000	0.477	-2.000	1.230	0.778
Average	0.523	-0.891	0.255	0.678	2.087	0.057	-0.630	1.274	1.770	1.472	0.686	1.373	-1.396	-0.485	2.753	0.019	-1.954	1.456	2.583	0.825	-1.583	0.175	0.692	1.678	-1.111	2.142	1.811
Std_dev	1.102	0.382	0.232	0.728	0.342	0.261	0.303	0.228	0.380	0.353	0.168	0.726	0.253	0.284	0.252	0.371	0.129	0.384	0.229	0.364	0.724	0.403	0.240	0.329	0.450	0.283	0.223

Cov_mat	Au	Ag	Al	As	Ba	Bi	Ca	Co	Cr	Cu	Fe	Hg	K	Mg	Mn	Mo	Na	Ni	P	Pb	S	Sb	Sc	Sr	Ti	V	Zn
Au	1.214	0.259	-0.098	0.496	-0.119	0.105	-0.064	-0.037	-0.039	0.181	-0.009	0.463	-0.016	-0.003	-0.103	0.173	-0.020	0.014	-0.012	0.176	0.360	0.194	-0.083	-0.120	-0.231	-0.117	-0.011
Ag	0.259	0.146	-0.022	0.168	-0.021	0.052	-0.019	-0.016	-0.031	0.073	0.002	0.158	0.013	-0.004	-0.034	0.064	-0.005	-0.016	0.008	0.060	0.123	0.079	-0.024	-0.030	-0.064	-0.032	0.007
Al	-0.098	-0.022	0.054	-0.047	0.054	-0.015	0.030	0.027	0.020	0.000	0.007	-0.008	0.024	0.022	0.033	-0.027	0.003	0.025	0.014	-0.005	-0.052	-0.027	0.047	0.046	0.035	0.019	0.015
As	0.496	0.168	-0.047	0.529	-0.024	0.080	-0.019	-0.022	-0.030	0.165	0.008	0.341	0.036	-0.019	-0.072	0.120	-0.007	0.007	0.021	0.127	0.280	0.137	-0.042	-0.024	-0.161	-0.069	0.007
Ba	-0.119	-0.021	0.054	-0.024	0.117	-0.002	0.039	0.024	0.025	0.023	0.017	0.011	0.053	-0.004	0.036	-0.002	0.003	0.019	0.041	0.014	-0.021	0.005	0.044	0.089	0.042	0.033	0.019
Bi	0.105	0.052	-0.015	0.080	-0.002	0.068	-0.026	-0.013	-0.008	0.066	0.003	0.051	-0.005	-0.019	-0.028	0.048	-0.002	-0.010	0.000	0.035	0.057	0.082	-0.016	-0.009	-0.025	-0.014	-0.003
Ca	-0.064	-0.019	0.030	-0.019	0.039	-0.026	0.092	0.032	0.034	-0.007	0.006	0.017	0.032	0.045	0.037	-0.041	0.010	0.046	0.042	-0.017	-0.011	-0.040	0.030	0.071	0.024	0.022	0.020
Co	-0.037	-0.016	0.027	-0.022	0.024	-0.013	0.032	0.052	0.065	0.002	0.020	-0.001	0.004	0.038	0.045	-0.033	-0.001	0.066	0.012	-0.008	-0.037	-0.018	0.035	0.025	0.049	0.037	0.033
Cr	-0.039	-0.031	0.020	-0.030	0.025	-0.008	0.034	0.065	0.144	0.004	0.027	-0.029	-0.009	0.047	0.041	-0.032	-0.004	0.126	0.002	-0.011	-0.036	-0.008	0.039	0.038	0.067	0.053	0.028
Cu	0.181	0.073	0.000	0.165	0.023	0.066	-0.007	0.002	0.004	0.125	0.020	0.120	0.015	-0.004	-0.021	0.075	-0.003	0.012	0.025	0.074	0.110	0.098	0.002	0.016	-0.041	-0.007	0.022
Fe	-0.009	0.002	0.007	0.008	0.017	0.003	0.006	0.020	0.027	0.020	0.028	0.009	0.005	0.003	0.016	0.009	-0.001	0.015	0.015	0.011	0.006	0.014	0.011	0.012	0.043	0.038	0.030
Hg	0.463	0.158	-0.008	0.341	0.011	0.051	0.017	-0.001	-0.029	0.120	0.009	0.527	0.045	-0.003	-0.035	0.078	-0.009	0.002	0.038	0.107	0.215	0.101	-0.011	0.004	-0.109	-0.042	0.015
K	-0.016	0.013	0.024	0.036	0.053	-0.005	0.032	0.004	-0.009	0.015	0.005	0.045	0.064	0.005	0.011	0.007	0.005	-0.001	0.033	0.014	0.035	0.002	0.013	0.046	-0.006	0.004	0.011
Mg	-0.003	-0.004	0.022	-0.019	-0.004	-0.019	0.045	0.038	0.047	-0.004	0.003	-0.003	0.005	0.081	0.032	-0.039	0.001	0.076	0.004	-0.030	-0.022	-0.033	0.031	0.009	0.006	0.005	0.021
Mn	-0.103	-0.034	0.033	-0.072	0.036	-0.028	0.037	0.045	0.041	-0.021	0.016	-0.035	0.011	0.032	0.064	-0.045	0.001	0.039	0.017	-0.015	-0.069	-0.036	0.039	0.030	0.064	0.042	0.032
Mo	0.173	0.064	-0.027	0.120	-0.002	0.048	-0.041	-0.033	-0.032	0.075	0.009	0.078	0.007	-0.039	-0.045	0.138	-0.008	-0.037	0.007	0.070	0.146	0.097	-0.029	-0.013	-0.057	-0.024	-0.005
Na	-0.020	-0.005	0.003	-0.007	0.003	-0.002	0.010	-0.001	-0.004	-0.003	-0.001	-0.009	0.005	0.001	0.001	-0.008	0.017	-0.004	0.008	-0.008	0.000	-0.005	0.001	0.009	0.011	0.004	0.001
Ni	0.014	-0.016	0.025	0.007	0.019	-0.010	0.046	0.066	0.126	0.012	0.015	0.002	-0.001	0.076	0.039	-0.037	-0.004	0.147	0.001	-0.017	-0.016	-0.016	0.041	0.032	0.019	0.021	0.025
P	-0.012	0.008	0.014	0.021	0.041	0.000	0.042	0.012	0.002	0.025	0.015	0.038	0.033	0.004	0.017	0.007	0.008	0.001	0.052	0.014	0.037	0.007	0.013	0.046	0.014	0.020	0.021
Pb	0.176	0.060	-0.005	0.127	0.014	0.035	-0.017	-0.008	-0.011	0.074	0.011	0.107	0.014	-0.030	-0.015	0.070	-0.008	-0.017	0.014	0.132	0.102	0.067	-0.006	0.009	-0.038	-0.009	0.010
S	0.360	0.123	-0.052	0.280	-0.021	0.057	-0.011	-0.037	-0.036	0.110	0.006	0.215	0.035	-0.022	-0.069	0.146	0.000	-0.016	0.037	0.102	0.416	0.112	-0.055	-0.015	-0.142	-0.059	0.005
Sb	0.194	0.079	-0.027	0.137	0.005	0.082	-0.040	-0.018	-0.008	0.098	0.014	0.101	0.002	-0.033	-0.036	0.097	-0.005	-0.016	0.007	0.067	0.112	0.162	-0.025	-0.008	-0.028	-0.009	0.003
Sc	-0.083	-0.024	0.047	-0.042	0.044	-0.016	0.030	0.035	0.039	0.002	0.011	-0.011	0.013	0.031	0.039	-0.029	0.001	0.041	0.013	-0.006	-0.055	-0.025	0.058	0.037	0.041	0.025	0.018
Sr	-0.120	-0.030	0.046	-0.024	0.089	-0.009	0.071	0.025	0.038	0.016	0.012	0.004	0.046	0.009	0.030	-0.013	0.009	0.032	0.046	0.009	-0.015	-0.008	0.037	0.108	0.038	0.031	0.014
Ti	-0.231	-0.064	0.035	-0.161	0.042	-0.025	0.024	0.049	0.067	-0.041	0.043	-0.109	-0.006	0.006	0.064	-0.057	0.011	0.019	0.014	-0.038	-0.142	-0.028	0.041	0.038	0.203	0.112	0.050
V	-0.117	-0.032	0.019	-0.069	0.033	-0.014	0.022	0.037	0.053	-0.007	0.038	-0.042	0.004	0.005	0.042	-0.024	0.004	0.021	0.020	-0.009	-0.059	-0.009	0.025	0.031	0.112	0.080	0.043
Zn	-0.011	0.007	0.015	0.007	0.019	-0.003	0.020	0.033	0.028	0.022	0.030	0.015	0.011	0.021	0.032	-0.005	0.001	0.025	0.021	0.010	0.005	0.003	0.018	0.014	0.050	0.043	0.050

Cor_mat	Au	Ag	Al	As	Ba	Bi	Ca	Co	Cr	Cu	Fe	Hg	K	Mg	Mn	Mo	Na	Ni	P	Pb	S	Sb	Sc	Sr	Ti	V	Zn
Au	1.000	0.616	-0.381	0.619	-0.316	0.364	-0.193	-0.146	-0.094	**0.464**	-0.049	0.578	-0.058	-0.011	-0.372	0.424	-0.139	0.033	-0.047	0.438	0.506	0.438	-0.314	-0.331	-0.466	-0.375	-0.045
Ag	**0.616**	1.000	-0.250	0.605	-0.160	0.519	-0.165	-0.185	-0.214	**0.539**	0.029	0.570	0.137	-0.034	-0.349	0.454	-0.102	-0.111	0.086	0.433	0.501	0.512	-0.259	-0.235	-0.372	-0.298	0.079
Al	-0.381	-0.250	1.000	-0.275	0.674	-0.245	0.430	0.501	0.222	-0.002	0.171	-0.048	0.400	0.337	0.566	-0.310	0.109	0.275	0.259	-0.063	-0.345	-0.284	0.849	0.602	0.337	0.291	0.283
As	**0.619**	0.605	-0.275	1.000	-0.098	0.422	-0.087	-0.130	-0.107	**0.641**	0.068	0.645	0.197	-0.091	-0.392	0.445	-0.071	0.025	0.127	0.481	0.596	0.467	-0.240	-0.098	-0.492	-0.334	0.040
Ba	-0.316	-0.160	0.674	-0.098	1.000	-0.027	0.375	0.312	0.195	0.188	0.293	0.045	0.611	-0.039	0.420	-0.018	0.072	0.146	0.526	0.115	-0.094	0.038	0.532	0.789	0.273	0.339	0.247
Bi	0.364	0.519	-0.245	0.422	-0.027	1.000	-0.325	-0.221	-0.076	**0.710**	0.072	0.271	-0.071	-0.257	-0.422	0.497	-0.060	-0.094	-0.003	0.371	0.337	0.776	-0.247	-0.100	-0.215	-0.185	-0.045
Ca	-0.193	-0.165	0.430	-0.087	0.375	-0.325	1.000	0.460	0.299	-0.061	0.108	0.077	0.412	0.526	0.489	-0.362	0.247	0.393	0.605	-0.150	-0.055	-0.329	0.417	0.715	0.177	0.254	0.289
Co	-0.146	-0.185	0.501	-0.130	0.312	-0.221	0.460	1.000	0.749	0.020	0.531	-0.007	0.061	0.593	0.784	-0.389	-0.018	0.754	0.226	-0.091	-0.254	-0.191	0.643	0.330	0.478	0.579	0.638
Cr	-0.094	-0.214	0.222	-0.107	0.195	-0.076	0.299	0.749	1.000	0.026	0.430	-0.106	-0.089	0.437	0.432	-0.230	-0.073	0.865	0.027	-0.082	-0.147	-0.049	0.423	0.300	0.389	0.490	0.328
Cu	**0.464**	0.539	-0.002	0.641	0.188	0.710	-0.061	0.020	0.026	1.000	0.345	0.469	0.167	-0.035	-0.232	0.575	-0.072	0.089	0.305	0.574	0.483	0.687	0.018	0.140	-0.256	-0.074	0.273
Fe	-0.049	0.029	0.171	0.068	0.293	0.072	0.108	0.531	0.430	0.345	1.000	0.075	1.000	0.247	-0.017	-0.194	0.288	-0.098	0.007	0.228	0.407	0.458	0.344	-0.062	0.018	-0.333	-0.206	0.095
Hg	**0.578**	0.570	-0.048	0.645	0.045	0.271	0.077	-0.007	-0.106	**0.469**	0.075	1.000	0.247	-0.017	-0.194	0.288	-0.098	0.007	0.228	0.407	0.458	0.344	-0.062	0.018	-0.333	-0.206	0.095
K	-0.058	0.137	0.400	0.197	0.611	-0.071	0.412	0.061	-0.089	0.167	0.118	0.247	1.000	0.064	0.164	0.074	0.150	-0.012	0.569	0.153	0.216	0.021	0.217	0.550	-0.054	0.058	0.201
Mg	-0.011	-0.034	0.337	-0.091	-0.039	-0.257	0.526	0.593	0.437	-0.035	0.060	-0.017	0.064	1.000	0.452	-0.366	0.030	0.700	0.061	-0.290	-0.120	-0.291	0.451	0.098	0.048	0.065	0.327
Mn	-0.372	-0.349	0.566	-0.392	0.420	-0.422	0.489	0.784	0.432	-0.232	0.372	-0.194	0.164	0.452	1.000	-0.485	0.041	0.408	0.289	-0.168	-0.424	-0.358	0.637	0.367	0.565	0.592	0.573
Mo	**0.424**	0.454	-0.310	0.445	-0.018	0.497	-0.362	-0.389	-0.230	**0.575**	0.148	0.288	0.074	-0.366	-0.485	1.000	-0.163	-0.256	0.079	0.520	0.611	0.650	-0.323	-0.106	-0.343	-0.230	-0.058
Na	-0.139	-0.102	0.109	-0.071	0.072	-0.060	0.247	-0.018	-0.073	-0.072	-0.023	-0.098	0.150	0.030	0.041	-0.163	1.000	-0.079	0.255	-0.175	-0.005	-0.094	0.041	0.221	0.182	0.110	0.019
Ni	0.033	-0.111	0.275	0.025	0.146	-0.094	0.393	0.754	0.865	0.089	0.232	0.007	-0.012	0.700	0.408	-0.256	-0.079	1.000	0.016	-0.122	-0.063	-0.106	0.440	0.250	0.110	0.190	0.286
P	-0.047	0.086	0.259	0.127	0.526	-0.003	0.605	0.226	0.027	0.305	0.389	0.228	0.569	0.061	0.289	0.079	0.255	0.016	1.000	0.165	0.252	0.074	0.234	0.608	0.138	0.315	0.418
Pb	**0.438**	0.433	-0.063	0.481	0.115	0.371	-0.150	-0.091	-0.082	**0.574**	0.185	0.407	0.153	-0.290	-0.168	0.520	-0.175	-0.122	0.165	1.000	0.433	0.458	-0.068	0.073	-0.230	-0.091	0.126
S	**0.506**	0.501	-0.345	0.596	-0.094	0.337	-0.055	-0.254	-0.147	**0.483**	0.055	0.458	0.216	-0.120	-0.424	0.611	-0.005	-0.063	0.252	0.433	1.000	0.433	-0.353	-0.070	-0.488	-0.320	0.032
Sb	**0.438**	0.512	-0.284	0.467	0.038	0.776	-0.329	-0.191	-0.049	**0.687**	0.202	0.344	0.021	-0.291	-0.358	0.650	-0.094	-0.106	0.074	0.458	0.433	1.000	-0.262	-0.060	-0.152	-0.082	0.034
Sc	-0.314	-0.259	0.849	-0.240	0.532	-0.247	0.417	0.643	0.423	0.018	0.264	-0.062	0.217	0.451	0.637	-0.323	0.041	0.440	0.234	-0.068	-0.353	-0.262	1.000	0.473	0.382	0.363	0.338
Sr	-0.331	-0.235	0.602	-0.098	0.789	-0.100	0.715	0.330	0.300	0.140	0.219	0.018	0.550	0.098	0.367	-0.106	0.221	0.250	0.608	0.073	-0.070	-0.060	0.473	1.000	0.255	0.331	0.185
Ti	-0.466	-0.372	0.337	-0.492	0.273	-0.215	0.177	0.478	0.389	-0.256	0.567	-0.333	-0.054	0.048	0.565	-0.343	0.182	0.110	0.138	-0.230	-0.488	-0.152	0.382	0.255	1.000	0.881	0.495
V	-0.375	-0.298	0.291	-0.334	0.339	-0.185	0.254	0.579	0.490	-0.074	0.808	-0.206	0.058	0.065	0.592	-0.230	0.110	0.190	0.315	-0.091	-0.320	-0.082	0.363	0.331	0.881	1.000	0.684
Zn	-0.045	0.079	0.283	0.040	0.247	-0.045	0.289	0.638	0.328	0.273	0.787	0.095	0.201	0.327	0.573	-0.058	0.019	0.286	0.418	0.126	0.032	0.034	0.338	0.185	0.495	0.684	1.000

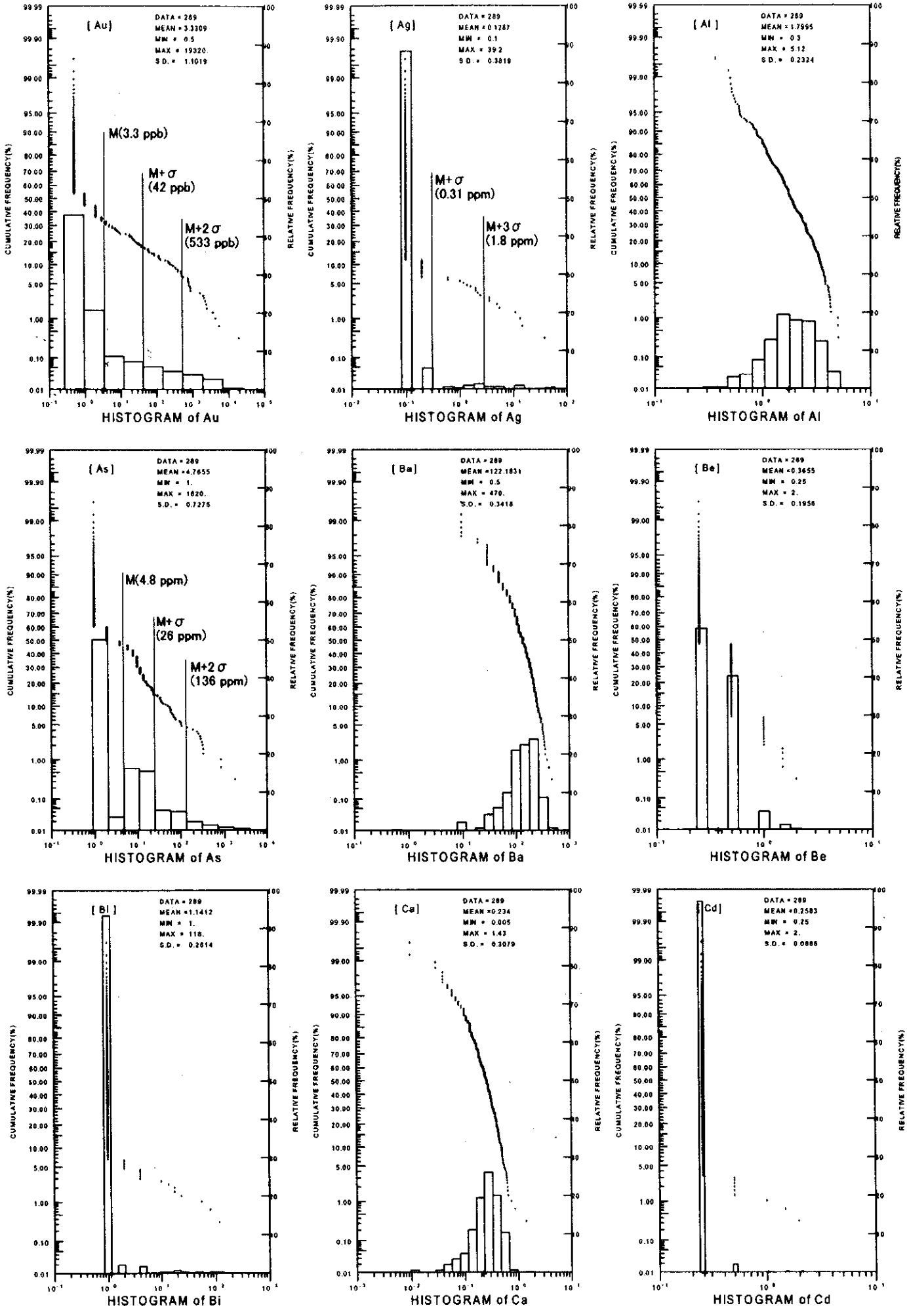

Fig. II-3-3 Probability plot of the Stream Sediments Samples (1)

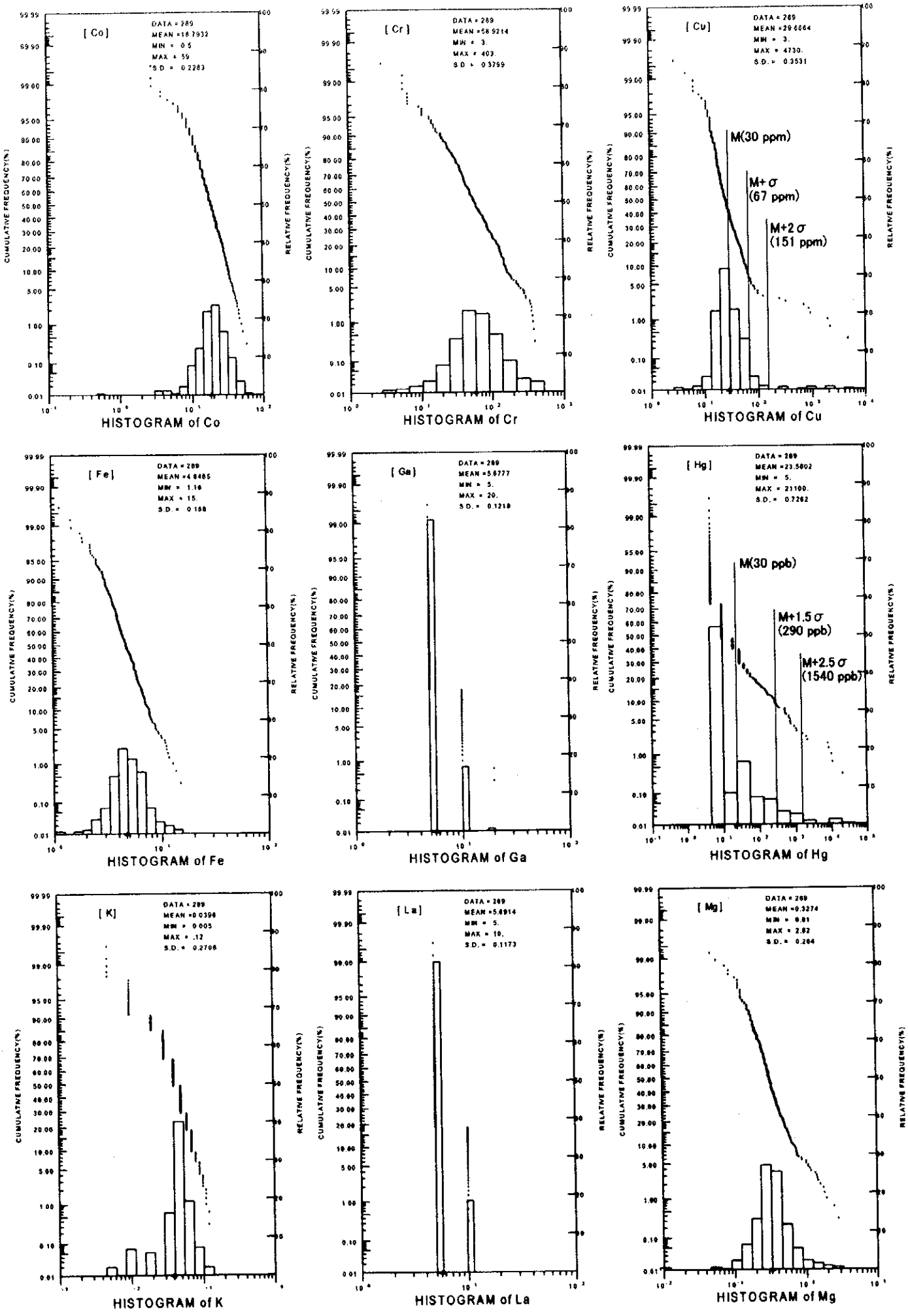

Fig. II-3-3 Probability Plot of the Stream Sediments Samples (2)

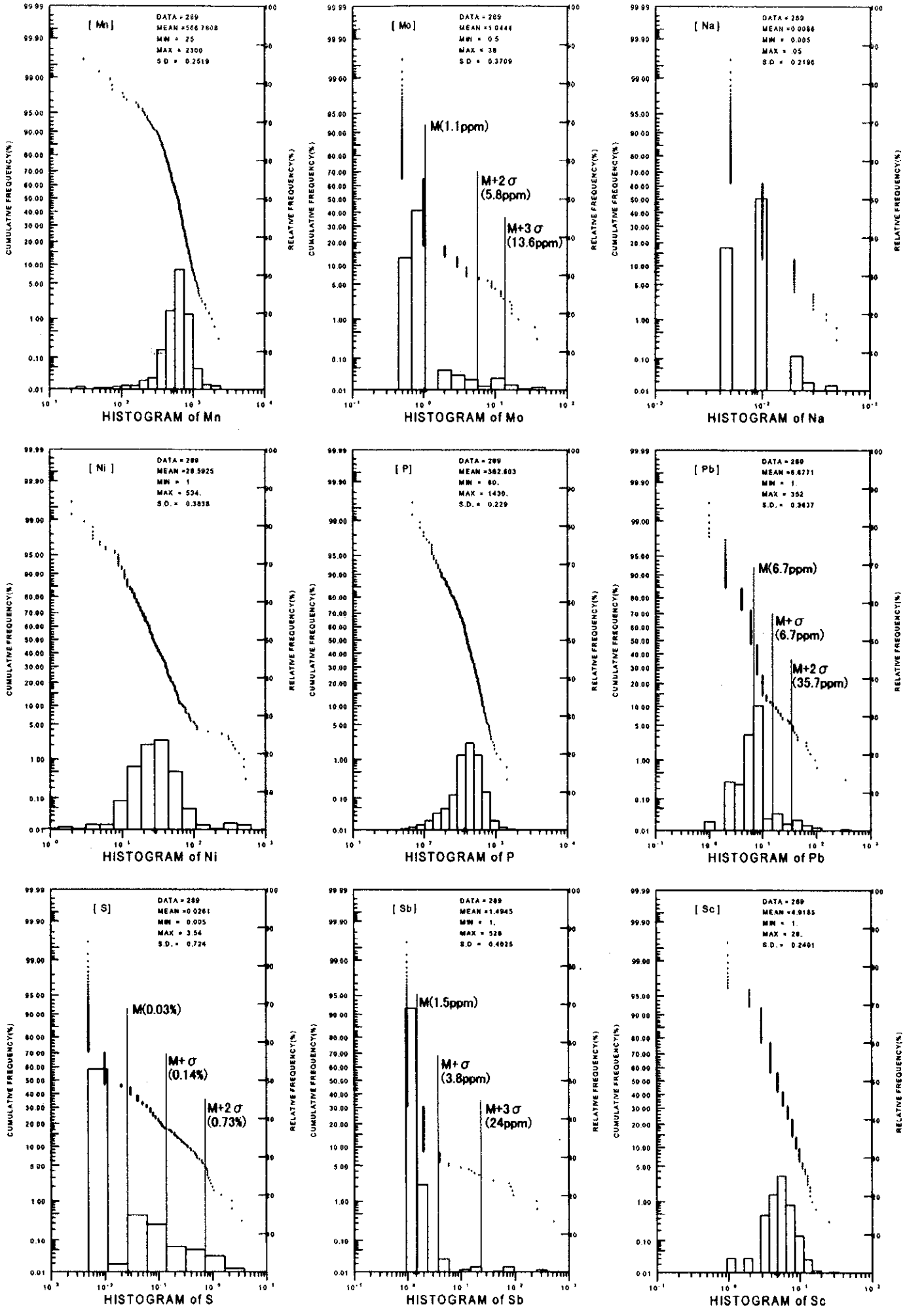

Fig. II-3-3 Probability Plot of Stream Sediments Samples (3)

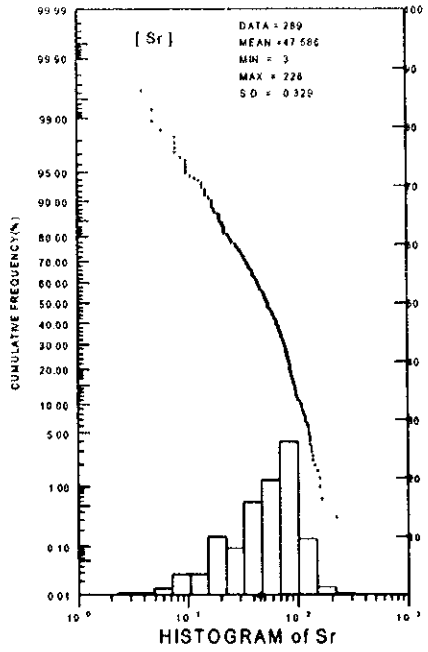

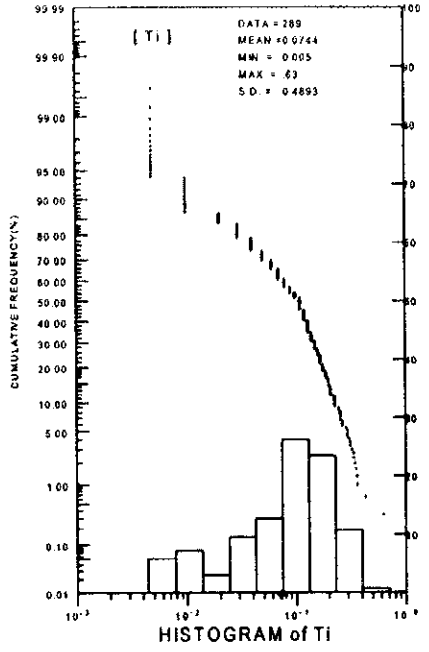

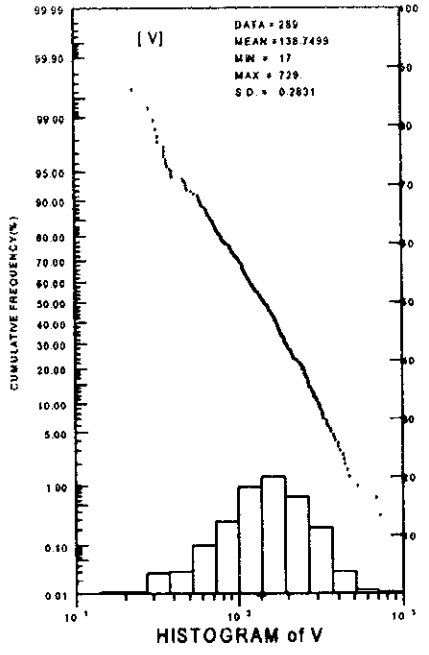

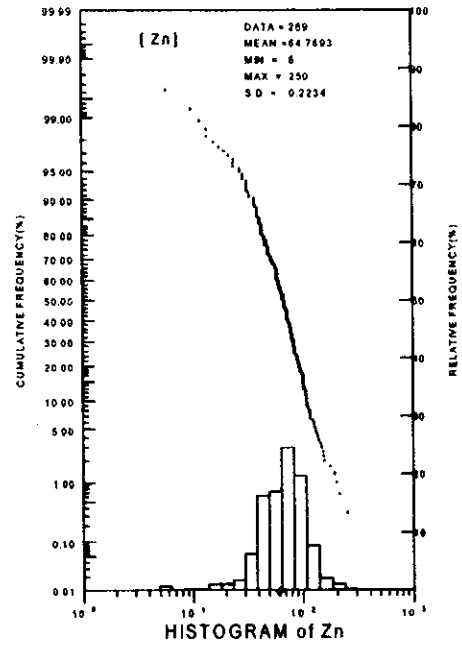

Fig. II-3-3 Probability Plot of Stream Sediments Samples (4)

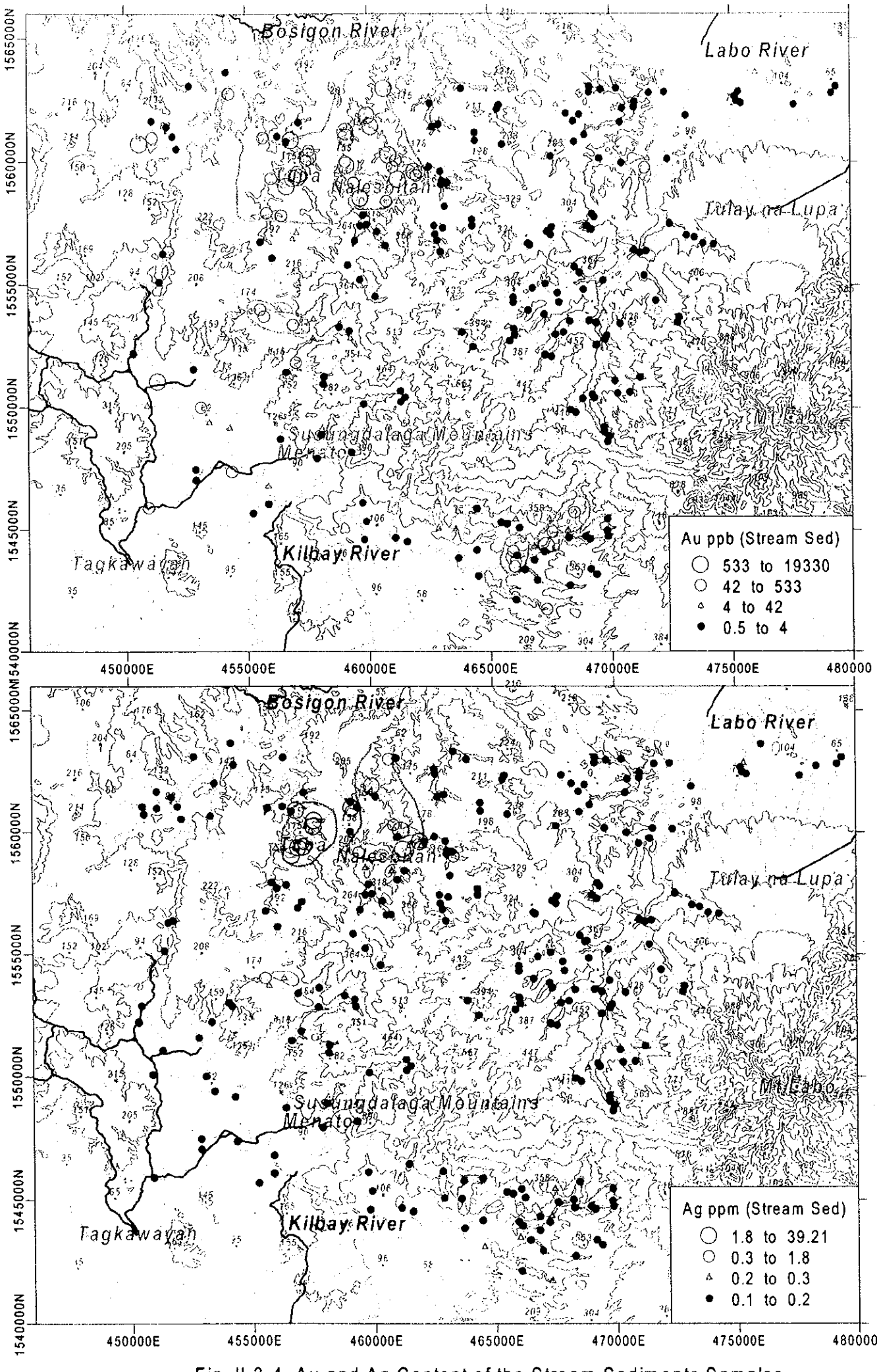

Fig. II-3-4 Au and Ag Content of the Stream Sediments Samples

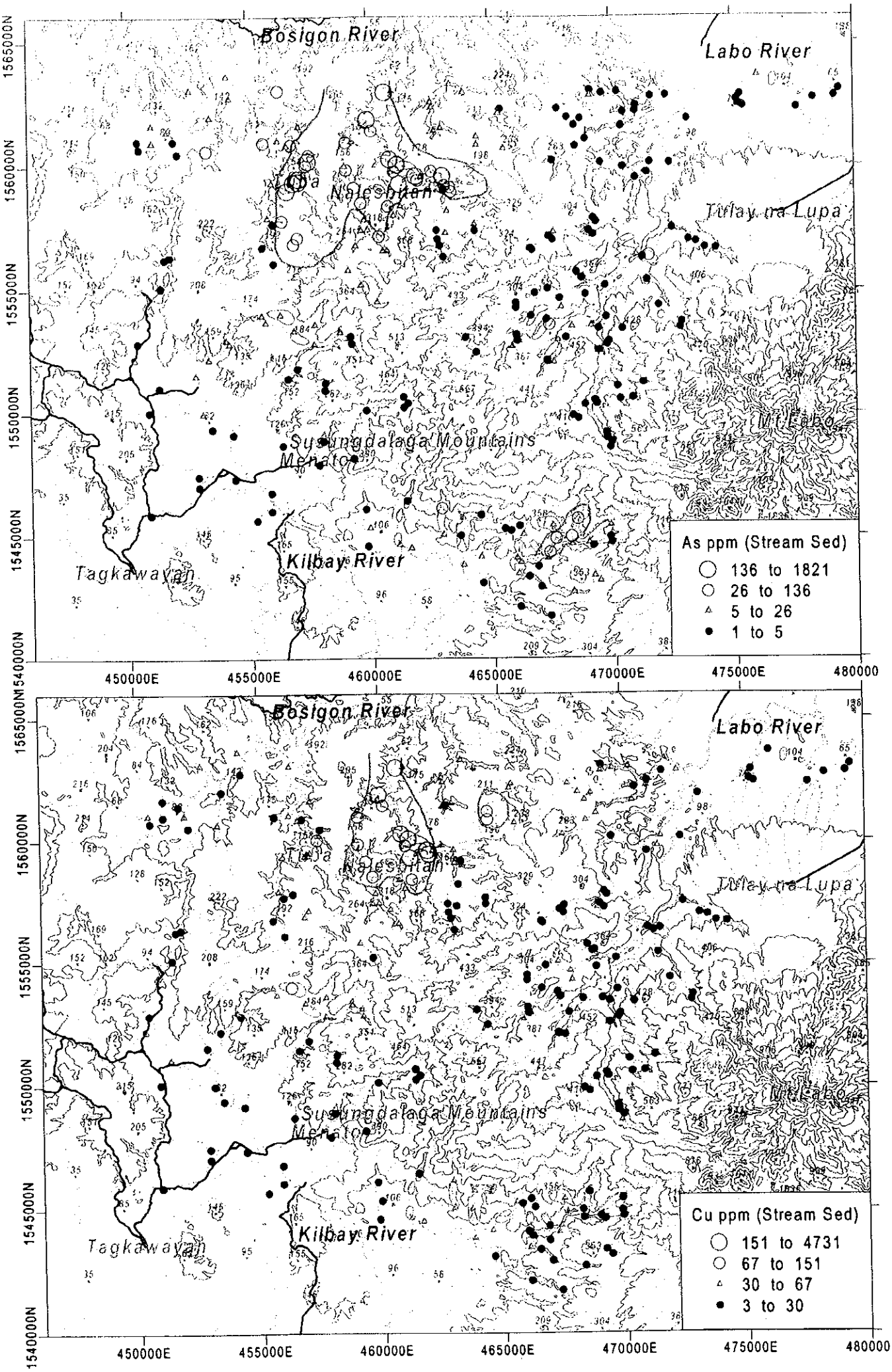

Fig. II-3-5 As and Cu Content of the Stream Sediments Samples

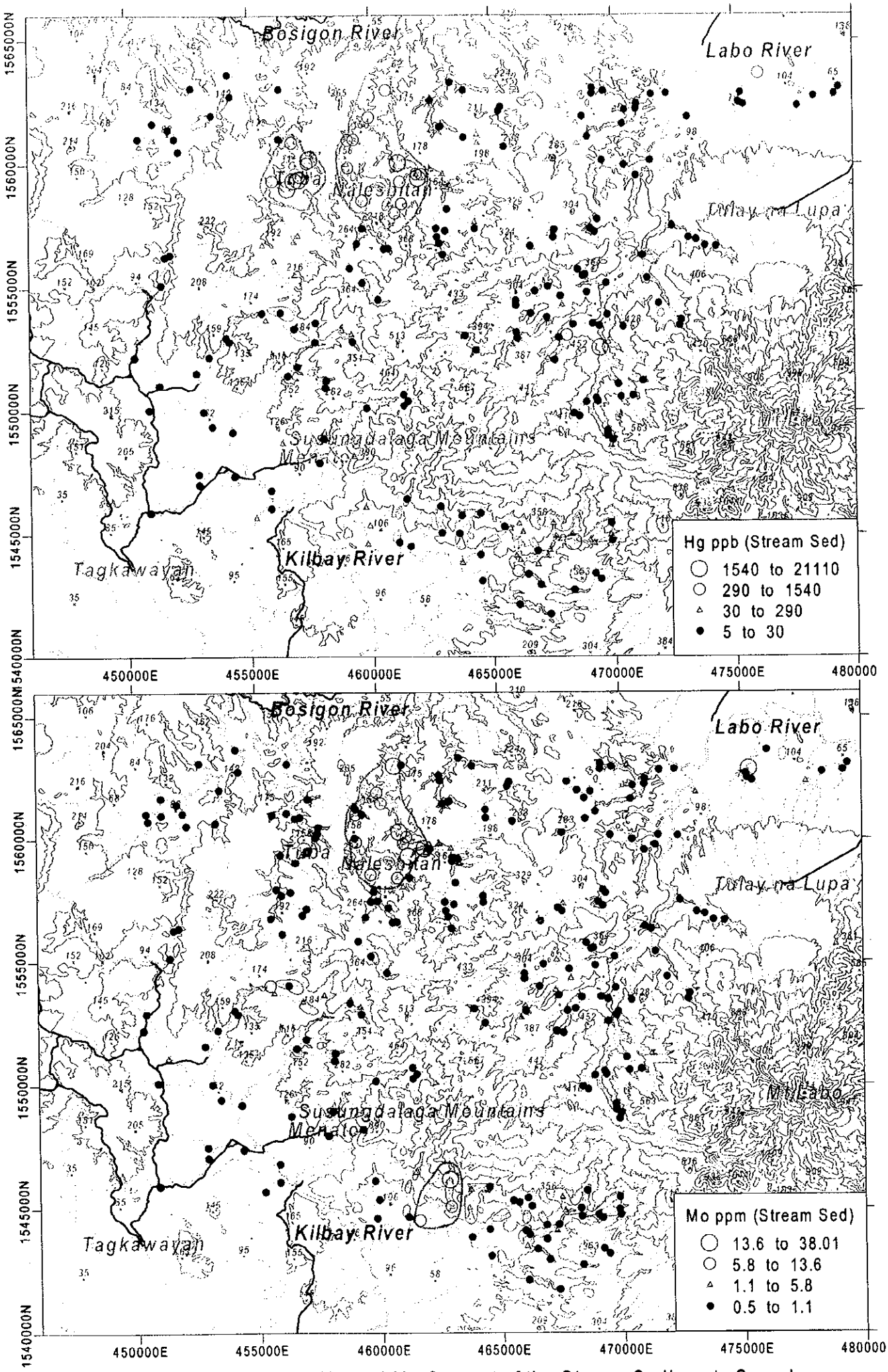

Fig. II-3-6 Hg and Mo Content of the Stream Sediments Samples

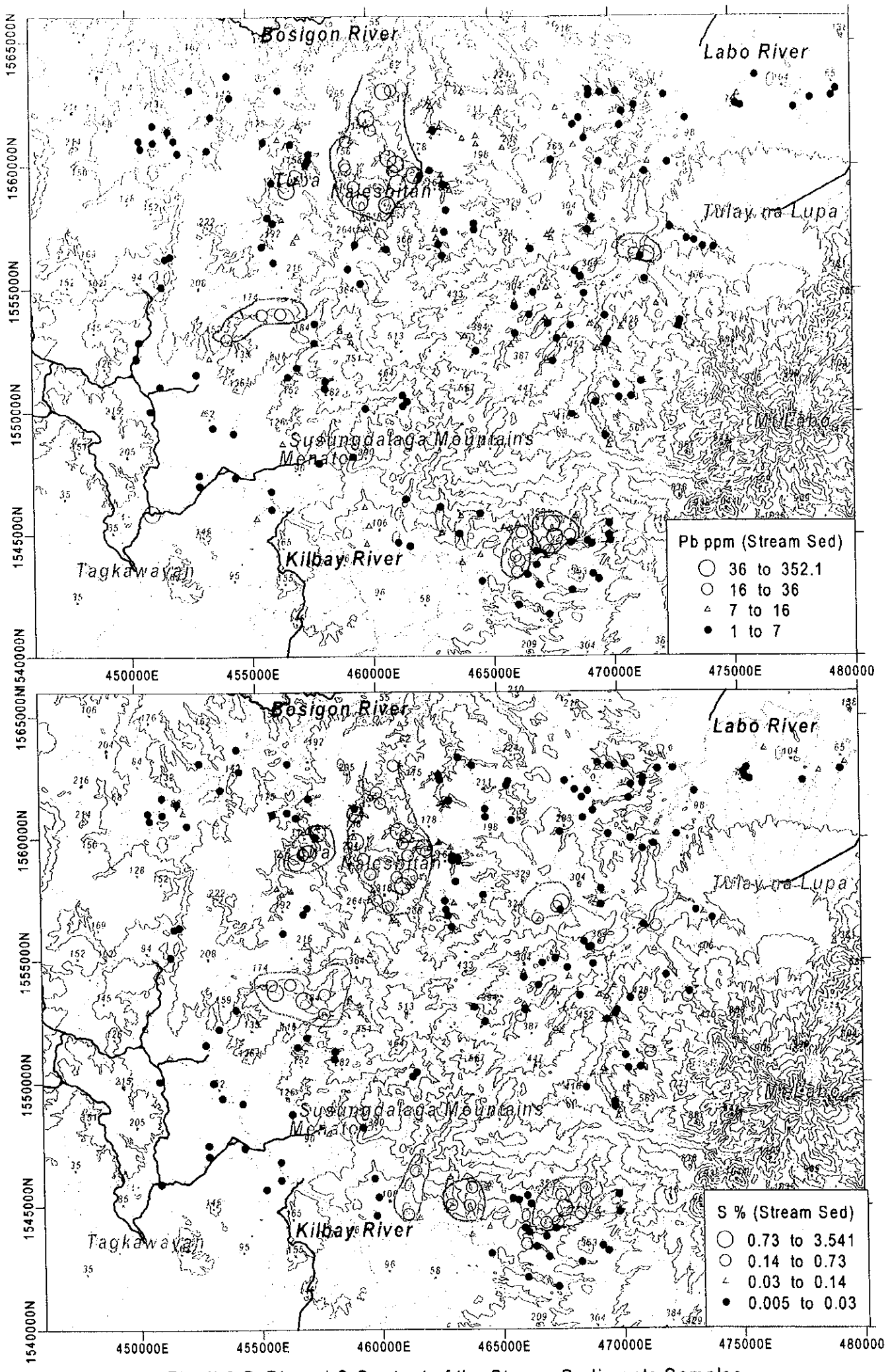

Fig. II-3-7 Pb and S Content of the Stream Sediments Samples

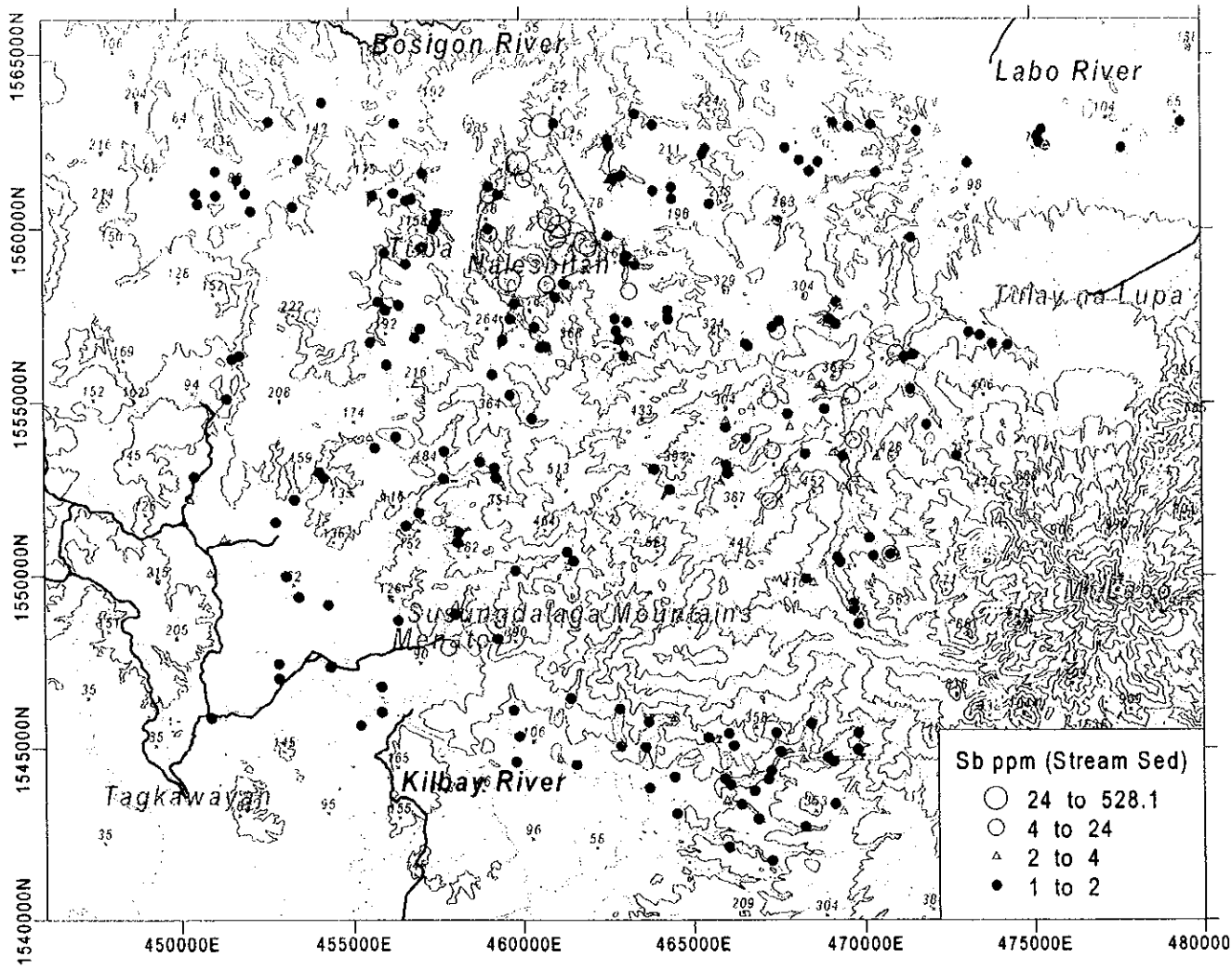

Fig. II-3-8 Sb Content of the Stream Sediments Samples

(2) Distribution of anomalies

In order to decide a threshold that sorts out an anomaly from a background level of geochemical data, various method have been proposed: an natural gap of probability curve, a inflection point of probability curve, a method to use average and standard deviation, a percentile of frequency distribution and others. In this paper, the combination of an average and a standard deviation is taken as a criterion. However, an inflection point and a natural gap are also considered for the decision. The threshold values of each element are shown on Fig.II-3-3.

The distribution of anomaly of each element is also shown in the content map of each element(Fig.II-3-4~II-3-8).

[Au] The samples with extremely high Au content concentrate in the area around Nalesbitan and Tuba mineral occurrences. The Alawihaw alteration zone in the upper part of Kilbay River and the Katakian alteration zone south of Tuba is also the areas with high gold content.
[Ag] The anomaly area is only confined the area around Nalesbitan and Tuba mineral occurrences.
[As] The samples with high As content concentrate in the area around Nalesbitan and Tuba mineral occurrences. This anomaly zone extends eastward to the Salobosogin-Yakalan alteration zone. The Alawihaw alteration zone is also the area with high As content. The anomalous values are scattered in the Maniknik alteration zone in the western tributary of Kilbay River, and the Magasawang Bato and the Taktak alteration zones in the upper stream of Labo River.
[Cu] The area with high Cu content is only confined in the area around the Nalesbitan mineral occurrences. The anomalous values are solely found in the Tuba occurrence and the Katakian alteration zone. It indicates that the Cu mineralization in Tuba is limited to a very small area. A cluster of anomalous values is detected 4 km east of Nalesbitan, but no indication was discovered by field mapping.
[Hg] The samples with high Hg content concentrate in the area around Nalesbitan and Tuba mineral occurrences. Some anomalous values are scattered in the upper stream of Kilbay River and the upper stream of Labo River.
[Mo] The samples with high Mo content concentrate in the Nalesbitan area and the Maniknik alteration zone.
[Pb] The samples with high Pb content concentrate in the Nalesbitan area, the northern part of the Katakian alteration zone, and the upper part of Kilbay River from Alawihaw to Katigbigan zone. The small anomaly zone is also detected in the Magasawang Bato alteration zone in Labo Valley.
[S] The sulfur content reflects directly the quantity of sulfide minerals in the collected stream sediments samples: especially the extension of the pyritization in the valley. The high sulfur zones are delineated in the Nalesbitan-Tuba area, the Katakian alteration zone, the area from Alawihaw to Katigbigan zone, the area from Layaton Malaki to Maniknik, and the Kampusta alteration zone.
[Sb] The samples with high Sb content concentrate in Nalesbitan area. Other high values are scattered in the upperstream of Labo River.

(3) Principal Components Analysis (PCA)

For the correlation matrix calculated from logarithm of analysis values of stream sediments samples, principal components values are calculated and the results are shown in Table II-3-2.

Table II-3-2 Result of Principal Component Analysis of the Stream Sediments Samples

Result of PCA

No.	Eig_value	Eig_%	Eig_sum
Z-01	8.070	29.890	29.890
Z-02	5.172	19.157	49.046
Z-03	2.725	10.093	59.139
Z-04	2.429	8.998	68.136
Z-05	1.467	5.433	73.570
Z-06	1.155	4.279	77.849
Z-07	0.948	3.512	81.361
Z-08	0.696	2.577	83.938
Z-09	0.635	2.350	86.288
Z-10	0.553	2.049	88.337
Z-11	0.448	1.660	89.997
Z-12	0.425	1.572	91.569
Z-13	0.353	1.306	92.875
Z-14	0.311	1.151	94.026
Z-15	0.271	1.003	95.030
Z-16	0.239	0.887	95.916
Z-17	0.215	0.795	96.711
Z-18	0.205	0.760	97.471
Z-19	0.147	0.545	98.016
Z-20	0.118	0.437	98.453
Z-21	0.099	0.367	98.820
Z-22	0.090	0.332	99.152
Z-23	0.077	0.285	99.437
Z-24	0.053	0.196	99.633
Z-25	0.040	0.149	99.781
Z-26	0.038	0.141	99.922
Z-27	0.021	0.078	100.000

Fact_Id	Z-01	Z-02	Z-03	Z-04	Z-05	Z-06	Z-07
Mn	**0.839**	0.141	-0.100	0.011	0.056	0.234	0.054
Co	**0.754**	0.368	-0.421	0.172	-0.014	0.046	0.015
Sc	**0.721**	0.258	0.050	0.167	-0.360	0.199	0.228
Ti	**0.690**	0.002	-0.184	-0.568	0.096	-0.031	0.135
V	**0.682**	0.242	-0.231	-0.573	0.198	-0.008	-0.046
Al	**0.682**	0.238	0.317	0.124	-0.375	0.231	0.260
Ca	**0.595**	0.299	0.312	0.405	0.282	-0.191	-0.082
Cr	**0.557**	0.268	-0.534	0.147	-0.193	-0.329	-0.265
Sr	**0.540**	0.440	**0.539**	0.029	-0.173	-0.257	-0.171
Bi	-0.538	0.434	-0.145	-0.214	-0.328	-0.315	0.302
S	-0.562	0.494	0.066	0.142	0.261	-0.123	-0.277
Ag	-0.576	0.496	-0.109	0.138	0.130	0.162	0.285
Au	-0.607	0.382	-0.280	0.295	0.142	0.114	0.057
Mo	-0.630	0.432	0.029	-0.254	-0.134	-0.046	-0.213
Cu	-0.367	**0.794**	-0.082	-0.050	-0.203	-0.106	0.158
P	0.278	**0.605**	0.459	-0.067	0.352	-0.103	-0.089
Fe	0.374	**0.582**	-0.339	-0.504	0.195	0.057	-0.100
Hg	-0.365	**0.575**	0.036	0.288	0.150	0.277	0.099
As	-0.561	**0.572**	-0.060	0.249	0.115	0.042	0.003
Pb	-0.388	**0.571**	0.027	-0.132	-0.161	0.262	-0.148
Zn	0.470	**0.555**	-0.304	-0.246	0.346	0.220	0.080
Sb	-0.532	**0.540**	-0.146	-0.300	-0.241	-0.240	0.119
K	0.176	0.480	**0.630**	0.121	0.097	0.113	-0.085
Ba	0.484	0.470	**0.513**	-0.142	-0.352	0.022	-0.088
Mg	0.481	0.124	-0.315	**0.642**	0.114	-0.049	0.170
Ni	0.486	0.290	-0.491	**0.510**	-0.179	-0.275	-0.160
Na	0.164	-0.013	0.328	-0.048	0.385	-0.517	0.487

Eig_vec	Z-01	Z-02	Z-03	Z-04	Z-05	Z-06	Z-07
Mn	0.295	0.062	-0.061	0.007	0.047	0.218	0.055
Co	0.266	0.162	-0.255	0.110	-0.011	0.043	0.016
Sc	0.254	0.113	0.031	0.107	-0.297	0.186	0.234
Ti	0.243	0.001	-0.112	-0.365	0.079	-0.029	0.139
V	0.240	0.106	-0.140	-0.368	0.164	-0.007	-0.048
Al	0.240	0.105	0.192	0.080	-0.310	0.215	0.267
Ca	0.209	0.131	0.189	0.260	0.233	-0.178	-0.084
Cr	0.196	0.118	-0.324	0.095	-0.159	-0.307	-0.272
Sr	0.190	0.193	0.326	0.019	-0.142	-0.239	-0.176
Bi	-0.189	0.191	-0.088	-0.137	-0.270	-0.293	0.310
S	-0.198	0.217	0.040	0.091	0.215	-0.115	-0.285
Ag	-0.203	0.218	-0.066	0.088	0.107	0.151	0.293
Au	-0.214	0.168	-0.170	0.189	0.117	0.106	0.058
Mo	-0.222	0.190	0.018	-0.163	-0.110	-0.043	-0.219
Cu	-0.129	0.349	-0.050	-0.032	-0.167	-0.099	0.162
P	0.098	0.266	0.278	-0.043	0.291	-0.096	-0.092
Fe	0.132	0.256	-0.205	-0.323	0.161	0.053	-0.102
Hg	-0.128	0.253	0.022	0.185	0.124	0.258	0.102
As	-0.198	0.252	-0.036	0.160	0.095	0.039	0.003
Pb	-0.137	0.251	0.017	-0.085	-0.133	0.244	-0.152
Zn	0.166	0.244	-0.184	-0.158	0.285	0.205	0.082
Sb	-0.187	0.238	-0.088	-0.193	-0.199	-0.223	0.122
K	0.062	0.211	0.382	0.078	0.080	0.106	-0.087
Ba	0.170	0.207	0.311	-0.091	-0.291	0.021	-0.091
Mg	0.169	0.055	-0.191	0.412	0.094	-0.046	0.174
Ni	0.171	0.128	-0.297	0.327	-0.147	-0.256	-0.165
Na	0.058	-0.006	0.199	-0.031	0.318	-0.481	0.500

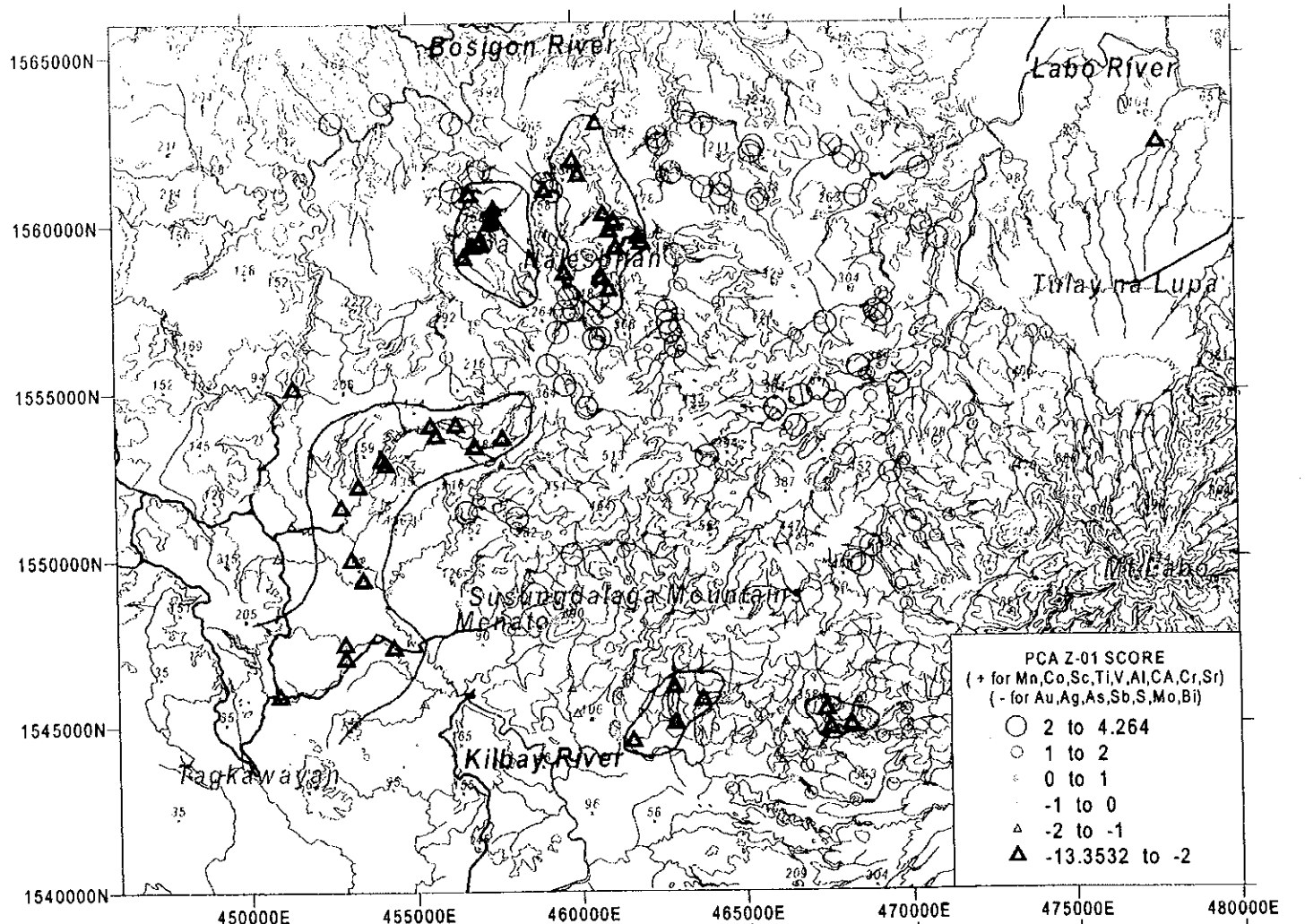

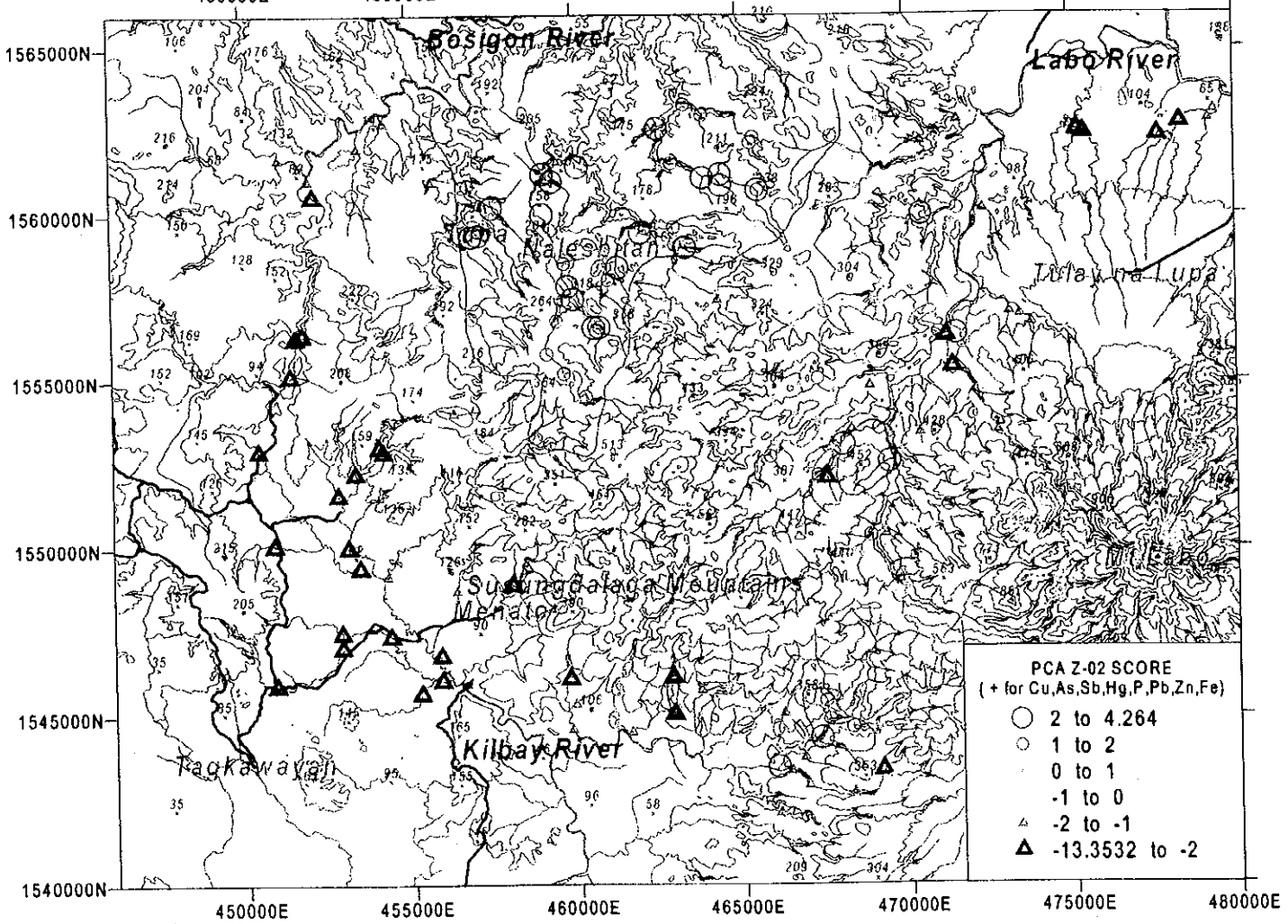

Fig. II-3-9 Z-01 and Z-02 PCA Score of the Stream Sediments Samples

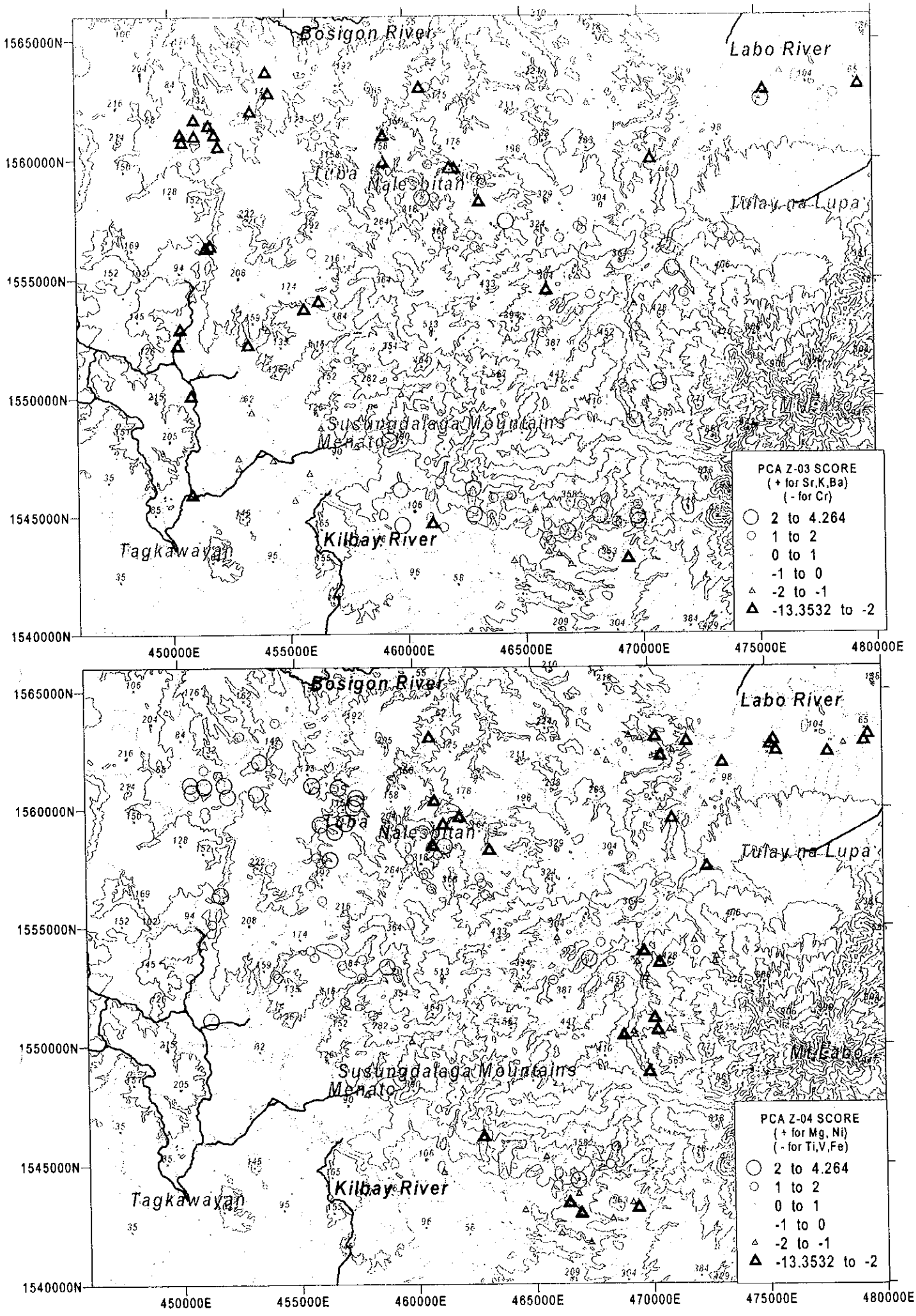

Fig. II-3-10 Z-03 and Z-04 PCA Score of the Stream Sediments Samples

Eigenvalues of up to the fourth principal components are above 2. Cumulative contribution up to the fourth principal components is 68%. The score distribution maps are shown in Fig.II-3-9~ II-3-10.

[Z-01] The factor loadings of Mn, Co, Sc, Ti, V, Al, Ca, Cr and Sr are highly positive. They are considered the correspondence to lithofacies of the survey area. Those of Au, Ag, As, Sb, Mo and Bi are negative. They are all pathfinder elements of epithermal mineralization, therefore it can be interpreted that the negative score represents a mineralization. The areas of negative scores are the area around Nalesbitan and Tuba deposits, the Katakian alteration zone, and the Alawihaw~ Katigbigan alteration zone, and the Layaton Malaki~Maniknik alteration zone. The Katakian alteration zone may become the source of a broad anomaly in the west part of the survey area.

[Z-02] The second principal component contributes 20% of original variability. The factor loadings of Cu, As, Sb, Hg, P, Pb, Zn and Fe are highly positive; therefore, it may indicate the Cu related mineralization. The areas of positive scores are around Nalesbitan and Tuba deposits, the Katakian alteration zone, and the Alawihaw~Katigbigan alteration zone, and the Magasawang Bato and the Binangkawan alteration zone in Labo Valley.

[Z-03] The third principal component contributes 10% of original variability. The factor loadings of Sr, K and Ba are positive, and it may indicate the quantity of plagioclase in the rock, while that of Cr is negative.

[Z-04] The fourth principal component contributes 9% of original variability. The factor loadings of Mg and Ni are positive, while those of Ti, V and Fe are negative. This component largely explains the lithofacies of the area. The area of positive scores is in the northwestern part, while that of negative scores is in the eastern part around Labo Valley.

3-3 Summary

The geochemical anomaly zones of each element are superimposed in Fig.II-3-11.

The Au anomalous values of the stream sediments samples are recognized in the following areas: Nalesbitan-Tuba mineral occurrences, the Katakian alteration zone and the Alawihaw alteration zone. It is seemed that some of the pervasive anomaly of Nalesbitan and Tuba is due to the contamination of mining activity, but taking the locations of the samples into consideration, the original anomaly may also extend widely around this area.

The sulfur anomaly zones, which may correspond to the volume of pyrite in the alteration zone, are outlined in Nalesbitan, Tuba, Katakian, the area around Alawihaw, Layaton-Maniknik, and Kampusta alteration zones.

The Mo anomaly zones are delineated in Nalesbitan area and the Maniknik alteration zone. The anomalous high Mo value in the Nalesbitan lodes were also reported by Sillitoe et al. (1990) and they suggested that acid-sulfate-type lode deposits containing Mo suite are characteristic of the upper part of porphyry Cu system. The Mo anomaly in Maniknik supports the possibility of the same type mineralization as Nalesbitan in this alteration zone.

The anomaly of the mobile elements such as Sb, As and Hg are often characterized the upper part of the epithermal systems. The anomalous values concentrate in the following areas: Nalesbitan, Tuba and the area around Alawihaw. The As anomaly in Nalesbitan extends eastward to the Salobosogin-Yakalan alteration zone. It may indicate the undiscovered Nalesbitan-type mineralized zone in this area. The anomalous values of Sb, As and Hg are scattered in the upper stream of

Kilbay River and the upper stream of Labo River.

The Z01 negative scores of PCA could outline the anomalies of Au related to pathfinder elements. The areas are Nalesbitan, Tuba, Katakian, Maniknik-Layaton, and the area around Alawihaw. The anomaly of the Katakian alteration zone extends broadly downstream in particular.

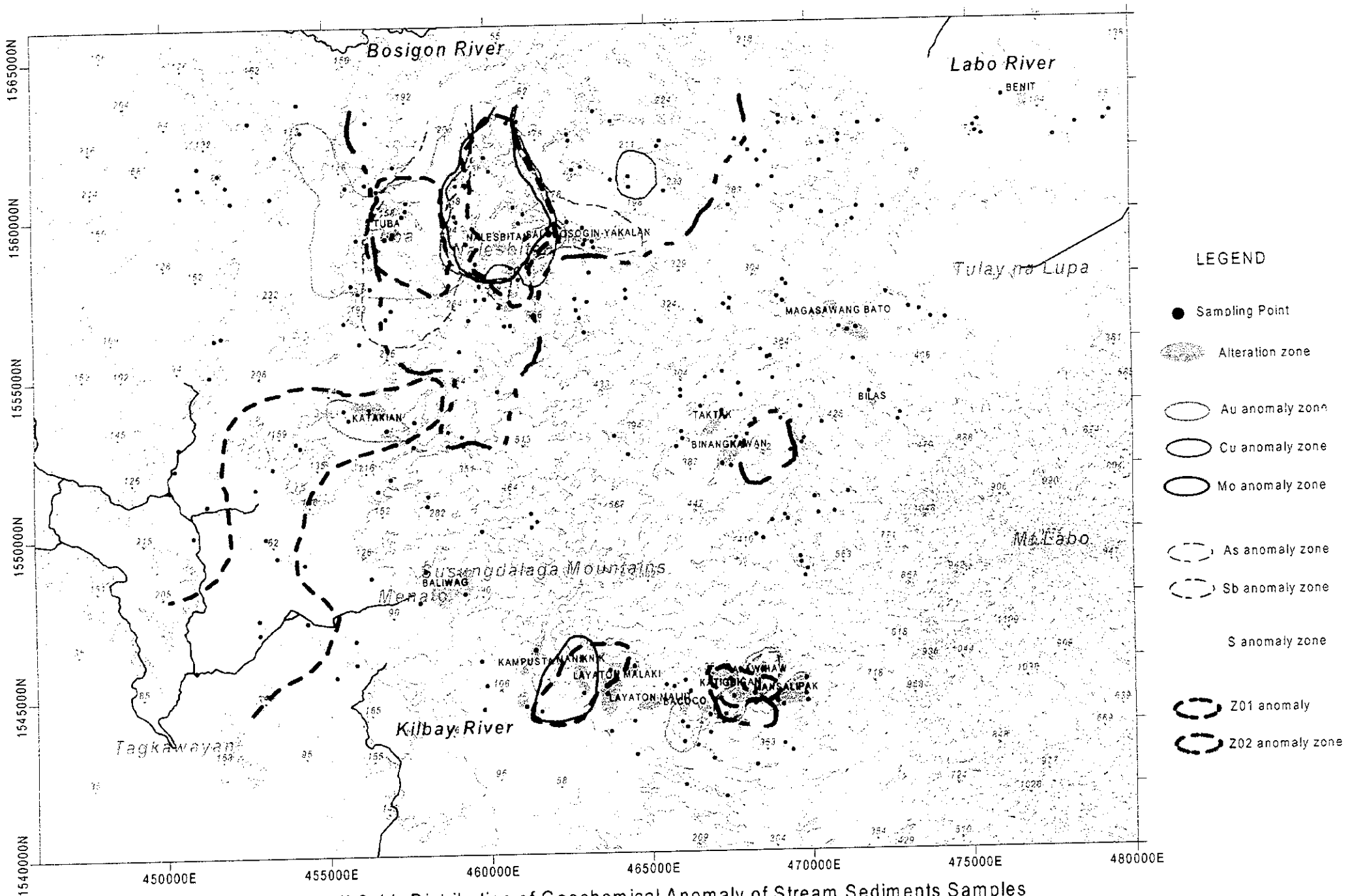

Fig. II-3-11 Distribution of Geochemical Anomaly of Stream Sediments Samples

Chapter 4 Discussion

4-1 Geologic structure, mineralization characteristics and control of the mineralization

The survey results are superimposed on Fig.II-4-1.

Field mapping, interpretation of airborne magnetic data, and digital terrain model show the dominance of northwest~west-northwest trending structures in the main part of the survey area belonging to the central zone. This trend is almost parallel to the WNW trending Legazpi Lineament situated in the south of Bicol Peninsula, and these structures accompany most of mineralization and alteration zones in the survey area.

Though no active mine is present in the survey area, Nalesbitan Au-Cu high sulfidation epithermal deposit and Tuba mesothermal vein-type deposit occur in the northwest of the area. In addition, Benit skarn-type small-scale deposit is present in the northeasternmost of the area. The mineralization of Nalesbitan is centered on a hydrothermal breccia in a dilational jog related to a northwest striking, sinistral strike-slip fault zone, with pervasive chalcedonic silicification and lack of vuggy residual silica.

In the survey area, there are many alteration zones besides the alteration haloes of Nalesbitan deposit and Tuba deposit.

The most pervasive alteration zone exposes along the Kilbay River's tributaries of the southern flank of the Susungdalaga Mountains in a corridor extending about 13 km from Alawihaw to Baliwag. It trends west-northwest and ranges 2 to 3 km wide. The east side of this zone nearby Alawihaw accompanies hot springs at high temperature, recent sinter terrace and sericite argillization with quartz-calcite veins. It means that this zone is formed by low-sulfidation system and is related to the active Labo geothermal field on the southwest flank of Mount Labo. The west side, Layaton Malaki-Maniknik-Baliwag area, provides a dominance of a silicified rock with partly vuggy texture containing alunite and enargite. This zone may have been produced by a high sulfidation system in relation to Pliocene volcanic activity.

The Katakian alteration zone south of Tuba deposit is characterized by silicification and sericitic argillization associated with quartz veins in the sedimentary rocks in the Tigbinan Formation, and it is inferred a vein-type mesothermal mineralization, which is similar to Tuba. However, the occurrences of magnetite veinlets and calc-silicate rocks nearby the intrusion of Paracale Granite may indicate a skarn-type mineralization. This alteration zone seems to be associated with northeast-trending faults rather than northwest-trending faults.

The Salobosogin-Yakalan alteration zone about 2 to 3 km east of the Nalesbitan deposit yields floats of vuggy chalcedonic quartz and is associated with northwest-trending fault. It appears that this zone is situated on the same geologic setting with Nalesbitan.

Other small alteration zones are observed around upperstream of Labo River. Some of these are accompanied by kaolinite argillization and possible steam heated alteration rocks. It may indicate the upper parts of the epithermal system.

4-2 Selection of promising areas

The targets in the survey area are epithermal to mesothermal gold±copper mineralizations. As the promising areas for further exploration, extensive alteration zone, geochemical anomaly of gold related elements, and broad high potassium gamma-ray spectral zone are overlapped. In addition, the existence of the related plugs and domes are necessary for the high sulfidation or porphyry Cu

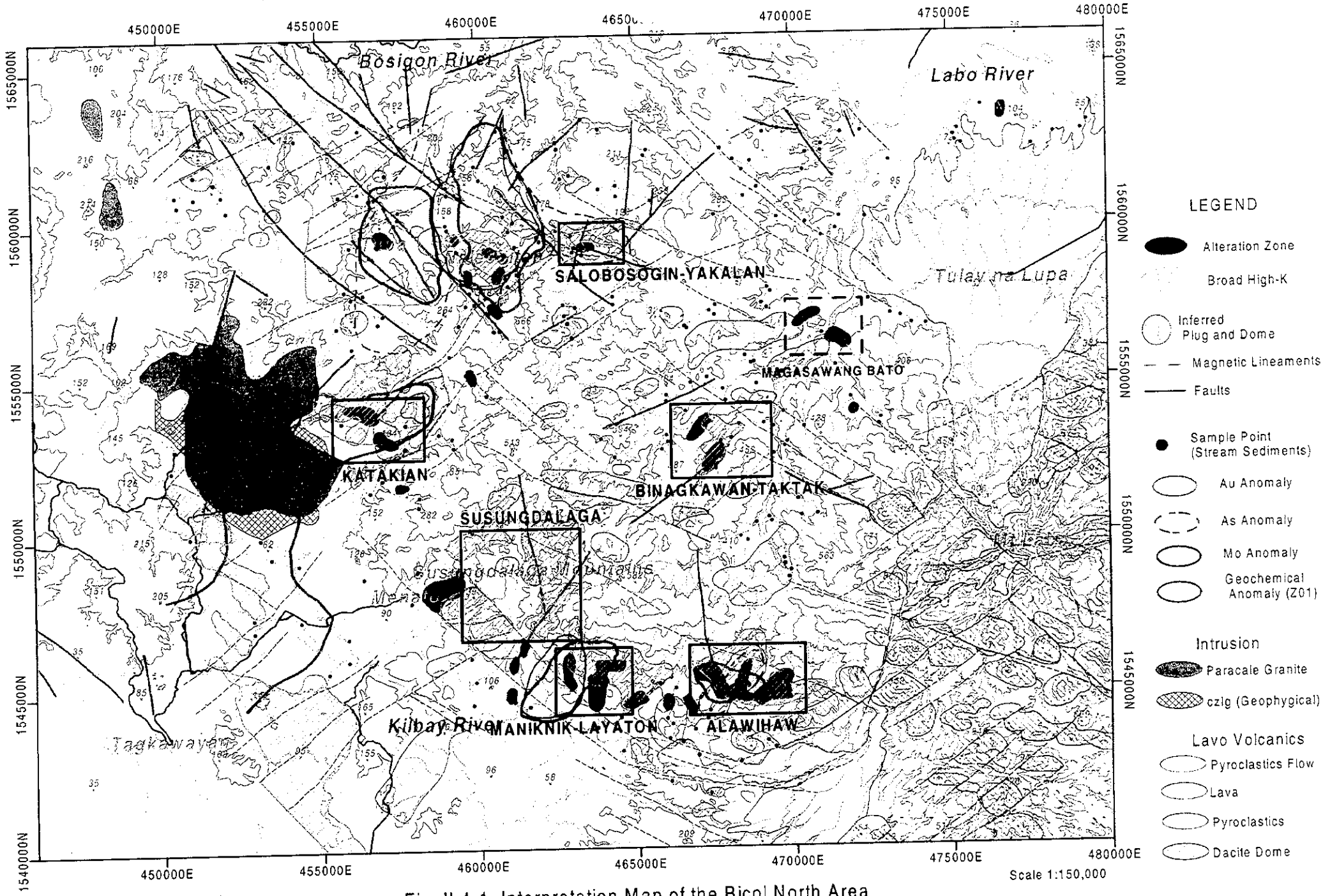

Fig. II-4-1 Interpretation Map of the Bicol North Area

mineralization. The following areas are consistent with above factors: the areas around Nalesbitan, Katakian, Maniknik-Layaton Malaki, and Alawihaw. In addition, the Salobosogin-Yakalan alteration zone, the Susungdalaga Area and the Binangkawan-Taktak alteration zone are included in these promising areas. Because the Salobosogin-Yakalan alteration zone has a broad high potassium anomaly and geochemical As anomaly. The Susungdalaga Area includes broad high potassium anomalies and inferred older volcanic eruptive center that may have been possible fluid source of the pervasive alteration of Kilbay River. No geochemical anomaly is detected in this area, but the density of geochemical samples is very low. Binangkawan-Taktak alteration zone which has a overlapping of kaolinite-smectite aleration zone and high potassium anomaly with an intersecition of NW trending structure and circular feature of the inferred Susungdalaga volcanic edifice determined by geophysical survey, but no remarkable geochemical anomaly, is also promising.

Nalesbitan has been already evaluated by many mining facilities, therefore any further exploration is no longer necessary in this project. The characteristic of these areas except Nalesbitan are described as follows:

(1) Katakian Alteration Zone

The alteration zone extends in the area of Cretaceous Tigbinan Formation and Pliocene Sta. Elena Formation. The Paracale Granite intrudes to the west of this zone on a large-scale, and the inferred another body intrude to the east of the area. The filed mapping is described silicification and sericitic argillization with quartz veins and abundant disseminated pyrite. Magnetite stringers and calc-silicate rocks is found on some outcrops. The geochemical anomaly of Au is detected and the anomaly of Au related elements extends broadly to downstream. The type of mineralization appears a skarn-type contact metasomatic mineralization related to plutonic bodies or mesothermal vein-type mineralization such as Tuba.

(2) Maniknik-Layaton Malaki Alteration Zone

The pervasive silicification in Pliocene Susungdalaga Volcanics is observed in this zone. The silicified rocks are accompanied by possible vuggy silica containing enargite in vugs and abundant alunite. These evidences show that this silicified zone was formed by typical high sulfidation type mineralization. The geochemistry of stream sediments reveals the anomaly of Au related elements and Mo in this area.

(3) Susungdalaga Area

The area is defined by broad high potassium gamma-ray anomalies extending from the Maniknik-Layaton alteration zone to north by 5 km. An inferred older volcanic eruptive center are expected resulting from airborne geophysical survey. No geochemical anomaly is detected in the stream sediments samples, but abundant silicified floats bearing Au were reported at Tonton River neighbor on the north of Baliwag Creek by JICA and MMAJ (1999). There is a possibility of high sulfidation mineralization in this area. Usually the potentiality of high sulfidation tends to become higher toward a volcanic center because of its necessity of the injection of magmatic fluid to the hydrothermal system. It has also a possibility that the pervasive alteration zone at the south flank of Susungdalaga Mountains was formed by a hydrothermal flow from this area.

(4) Salobosogin-Yakalan Alteration Zone

This alteration is related to northwest trending faults set cutting the Macogan Formation. The

broad high potassium gamma-ray anomaly zone is also detected along northwest trending faults delineated by airborne geophysical survey. Abundant silicified floats similar to those of Nalesbitan are observed along its creek, but the distribution is not clearly known. Only As anomaly is detected from stream sediments. This area may be expected a Nalesbitan-type mineralization associating with a dilational jog of fault system.

(5) Alawihaw Alteration Zone

The sericitic argillization and partly silicification in Pliocene Susungdalaga Volcanics are observed in this area. These rocks contain quartz veins and dissemination of pyrite. Hot springs at high temperature and recent silica-carbonate sinter terrace are also found in the alteration zone. It indicates that this alteration zone is formed by low-sulfidation system, and at least a part of this alteration zone is related to the active Labo geothermal field on the southwest flank of Mount Labo. The geochemical anomalies of Au, Cu and As are detected around this alteration zone.

(6) Binangkawan-Taktak Alteration zone

The details have not yet been known. But this area has a overlapping of kaolinite-smectite alteration zone and high potassium anomaly but no remarkable geochemical anomaly. An intersection of NW-trending structure and circular feature were determined by geophysical survey. This area is also interested.

The potentiality of other small alteration zones is briefly described as follows:

The area around Tuba deposit shows remarkable prominent geochemical anomaly by inferred contamination of small-scale mining activity, but no high potassium gamma-ray zone indicates the area is confined in a small area.

The Magasawang Bato alteration zone in the upper stream of Labo River shows no significant geochemical anomaly and lack of high potassium gamma-ray anomaly, but kaolinite argillization and possible steam heated alteration may indicate the upper parts of the epithermal system. In any case, this area becomes low priority: thereby this area shows as dotted boxes in Fig.II-4-1.

Part III

Conclusion and Proposal for the Third Phase Exploration

Part III Conclusion and Proposal for the Third Phase Exploration

Chapter 1 Conclusion

The interpretation of geophysical data, geological traverse and mapping, and geochemical prospecting of stream sediments are conducted in this Second Phase Program. The airborne magnetic and radiometric data were only acquired in the First Phase survey.

The main part of the survey area belongs to the central zone of three zones in Bicol area that is mainly covered by the Pliocene to Pleistocene volcanics. The area near Labo town consists of Paleogene sedimentary rocks, and the west and southwest parts are underlain by the ophiolite sequence and Cretaceous sedimentary rocks. Those areas belong to the northeast zone and the southwest zone.

In the field survey, many alteration zones are revealed including the alteration haloes of Nalesbitan deposit and Tuba deposit. Some parts of these alteration zone contains low- and high-epithermal, mesothermal vein-type, skarn-type mineralizations. The geochemical exploration is also revealed the geochemical haloes and anomalies related to these alteration zone.

In the geophysical interpretation, it has been on identifying the units based on a combination of their distinctive geophysical characteristics and possible eruptive centers are estimated in the Pliocene volcanics. The gamma-ray spectral data, in particular on potassium, outlines other areas of alteration in the study area. These possible alteration zones almost overlap with the geologically mapped alteration zones.

The following six promising areas for further exploration and its possible type of mineralization are selected from the results of this phase survey:

Katakian Alteration Zone – skarn-type or mesothermal vein-type deposits
Maniknik-Layaton Alteration Zone – high sulfidation epithermal deposits
Susungdalaga Area – high sulfidation epithermal deposits
Salobosogin-Yakalan Alteration Zone – high sulfidation epithermal deposits
Alawihaw Alteration Zone – low sulfidation epithermal deposits
Binangkawan-Taktak Alteration Zone-high or low sulfidation? epithermal deposits

Chapter 2 Proposal for the Third Phase Exploration

This second phase survey in the Bicol North area is, practically, the reconnaissance survey at a grass-route field due to its density of geologic mapping and geochemical sampling. Significant mineralization zones, where the drilling survey would be immediately necessary, have not been presently discovered, therefore further detailed geologic and geochemical survey are still necessary in the selected promising areas for the purpose of the decision for the drilling targets. The proposed third phase survey is as follows:

(1) Maniknik-Layaton Alteration Zone and (2) Susungdalaga Area

These areas have potentialities of high sulfidation mineralization. In a typical high-sulfidation mineralization accompanied by vuggy silica, the gold and its related elements usually concentrate

at the vuggy silica portion, the center of acidic alteration zone where acidic fluid directly ascended. However, vuggy silica bodies do not always contain high anomalous gold values, it certainly needs the ascent of metal rich fluid on and after the leaching process. Therefore, to check the existence of the gold mineralization, detailed geologic mapping and geochemical work including continuous rock chip sampling and/or channel sampling at vuggy silica bodies and silicified rocks is necessary. Once the mineralization will be discovered, geophysical survey is effective to outline the extension of the mineralization. It is expected that ore body and argillic zone surrounding silicified rock contains highly sulfide minerals, whereas silicified rock around vuggy silica, formed by the fluid descending temperature, shows high to medium resistivity and contains a little sulfide minerals. Therefore, it may be possible to detect the contrast by IP survey between both.

(3) Katakian Alteration Zone

This alteration zone appears to be accompanied by a skarn-type contact metasomatic mineralization related to plutonic bodies or mesothermal vein-type mineralization such as Tuba-type. The extension of quartz-vein outcrops and floats, silicified and argillic zone and geochemical anomalies will be determined by detailed mapping and geochemical work including detailed stream sediments sampling. Once the mineralization zones will be specified, grid soil sampling will be effective to decide the drilling target.

(4) Salobosogin-Yakalan Alteration Zone

This area has potentiality of Nalesbitan-type high sulfidation mineralization accompanied by silicified breccia. Only smectite dominant argillization crops out, many silicified boulders including some vuggy texture accumulate along the stream. Thereby, firstly the detailed field mapping is necessary to identify the extension of exposed silicified rocks. After that, geochemical work including continuous rock chip sampling and/or channel sampling every few to 10 meters intervals at vuggy silica and brecciated silicified bodies is necessary with paying special attention for brecciation and decomposed sulfide minerals. Au anomaly shows directly the mineralization. In addition, the mobile elements such as Hg, As and Sb are important, because this zone may only expose the shallow part of the system.

(5) Alawihaw Alteration Zone

It seems that this alteration zone was formed at a very shallow circumstance in a younger geothermal system due to the existence of sinter and active hot springs. The geochemical anomalies of mobile elements such as Hg, As and Sb are important to study a shallow system. The simultaneous detailed geologic mapping and rock-chip geochemical survey are recommended to specify the further promising area, then grid soil sampling will be carried out for the purpose of the decision of the drilling target.

However, the geothermal condition, the existence of hot springs at ~80℃, may interfere with the further survey including drillings.

(6) Binangkawan-Taktak Alteration zone

The existence of alteration zone has been determined but the details have not yet been known. At first, the detail geologic mapping and rock-chip geochemical survey are recommended to be done in parallel. In case any promising mineralization were found, grid soil sampling may be carried out in the area.

References

Bureau of Mines and Geosciences (1982): Geology and mineral resources of the Philippines, Vol 1, Geology, pp406, Bureau of Mines and Geo-Science, Ministry Nat. Resources, Manila, Philippines

Bureau of Mines and Geosciences (1986): Geology and mineral resources of the Philippines, Vol 2, Mineral Resources, pp446, Bureau of Mines and Geo-Science, Ministry Nat. Resources, Manila, Philippines

Caleon, P. C. (1970): Report on the geological investigation of the copper-lead prospect at Barrio Parang, Paracale, Camarines Norte. Bureau of Mines and Geo-Sciences internal report

Corbett, G.J. and Leach, T.M. (1994): SW Pacific Rim Au/Cu Systems: Structure, Alteration and Mineralisation. Notes from a Workshop Presented at Townsville, Australia, 28-29 Nov 1994

Dickson, B.L. and Scott, K.M. (1997): Interpretation of aerial gamma-ray surveys – adding the geochemical factors. AGSO Journal of Australian Geology and Geophysics 17 : 187 – 200

James, L.P. and Fuchs, W.A. (1990): Exploration of the Exicaban gold-copper-tellurium vein system, Camarines Norte, Philippines. Journal Geochemical Exploration 35 : 363-385

Japan International Cooperation Agency and Metal Mining Agency of Japan (1998): Report on Regional Survey for Mineral Resources in the Bicol Area, the Republic of the Philippines (Phase I)

Japan International Cooperation Agency and Metal Mining Agency of Japan (1999): Report on Regional Survey for Mineral Resources in the Bicol Area, the Republic of the Philippines, Final Report

McLennan, R. (1997): Nalesbitan Gold Project–Camarines Norte. Mining Philippines 97, 9-12 July, 17 pp

Miranda, F. E. and Caleon, P. C. (1979): Geology and mineral resources of Camarines Norte and parts of Quezon Province: Philippine Bureau of Mines Report of Investigation no.94

Mitchell, A.H.G. and Balce, G.R. (1990): Geological features of some epithermal gold systems, Philippines. Journal Geochemical Exploration 35 : 241-296

Mitchell, A.H.G. and Leach, T. M. (1991): Epithermal Gold in the Philippines: Island Arc Metallogenesis, Geothermal Systems and Geology. Academic Press, London, 457pp

Pubellier, M., Quebral, R., Aurelio, M. and Rangin, C. (1996): Docking and post-docking escape tectonics in the southern Philippines. In Hall, R and Blundell, D (eds) Tectonic Evolution of Southeast Asia, Geological Society Special Publication No 106, pp 511-523

Sillitoe, R.H., Angeles Jr, C.A., Comia, G.M., Antioquia, E.C. and Abeya, R.B. (1990): An acid-sulphate -type lode gold deposit at Nalesbitan, Luzon, Philippines. Journal Geochemical Exploration 35 : 387-411

United Nations (1987): Geology and Mineraliztion in the Panganiban-Tabas and Bulala areas, Camarines Norte. Techinical Report No.1, DP/UN/PHI-85-001/1, United Nations Development Program, New York, 43pp

White, N.C. and Hendenquist, J.W. (1990): Epithermal environments and styles of mineralization: variations and their causes, and guidelines for exploration. Journal Geochemical Exploration 36 : 445-474

Zaide-Delfin, M.C., Gerona, P.P., Layugan, D.B., Maturgo, O.O., Padua, D.O., Panem, C.C., Rosell, J.B. and Salonga, N.D.(1995): Mount Labo Geothermal Project Resource Assessment Update. PNOC Energy Development Corporation, Draft Report